Rough Surface Scattering Under Gaussian Beam Illumination and the Kirchhoff Approximation

by

Keith Allen Tyeryar

Thesis submitted to the Faculty of the
Virginia Polytechnic Institute and State University
in partial fulfillment of the requirements for the degree of
MASTER OF SCIENCE
in
Electrical Engineering

APPROVED:

G. S. Brown, Chairman

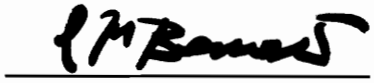

I. M. Besieris

W. L. Stutzman

May 26, 1993
Blacksburg, Virginia

c.2

Rough Surface Scattering Under Gaussian Beam Illumination and the Kirchhoff Approximation

by

Keith Allen Tyeryar

Committee Chair: Dr. Gary S. Brown

Electrical Engineering

(Abstract)

In this thesis, an analysis of the scattering of a rough perfect electric conductor (PEC) surface under illumination by a Gaussian beam using the Kirchhoff approximation is presented. The analysis assumes a source distribution which yields a Gaussian beam solution as a radiated field. This field is used to excite a current density on the surface using the Kirchhoff approximation. A vector potential approach utilizes this current to calculate the fields scattered by the surface. The analysis is carried out for the backscatter case and near normal incidence in order to reduce the final numerical evaluation to a two dimensional integration. The normalized radar cross section (NRCS) is calculated and compared with the result for plane wave illumination.

The analysis explores the effects of varying the source aperture size, rough surface correlation length and rms height on the NRCS. An asymptotic evaluation of the mean squared field is presented, as well as the mathematical form of the fourth moment of the scattered field. As a further study, the NRCS of a rough surface under a Gaussian tapered plane wave illumination is presented. The interplay of the beam spot and correlation length for such illuminated surfaces is discussed.

Acknowledgements

I first of all would like to dedicate this thesis to the memory of my father James R. Tyeryar (1937-1988), whose patience in answering my questions inspired me to never stop learning. I owe a great debt of gratitude to my mother for her support and help, especially through my college years.

Special thanks also go to my advisor, Dr. Brown, for his patience and help in teaching me the theory of electromagnetics. I want to thank Dr. Besieris, Dr. Stutzman, Dr. Davis and Dr. DeWolf all of whom I have taken courses from and have taught me the about the world of EM.

To my roommates: Dan Mauney, Ken Blackard, Mark McMulkin, Glen Shivel and Greg Stewart, thanks for putting up with me and keeping me sane. To my officemates: Mike Newkirk and especially David Kapp, I want to thank you for many hours of discussions and reviews.

Finally, I wish to thank my girlfriend Jessica Malone who has weathered the distance between us and never given up hope on me.

Table of Contents

List of Figures

Chapter 1

INTRODUCTION AND SUMMARY

The calculation of the field scattered by surfaces is a practical and highly investigated field of interest. Its applications range from detecting flaws in materials to the filtering of non-cooperative targets from surface clutter. There has been much work done in the calculation of radar cross sections of finite targets, i.e. planes, tanks, ships, and other scattering objects. Extended targets have also been investigated for the purpose of clutter estimation, for resolving targets from background terrain, as well as for the estimation of surface characteristics. This thesis explores finding the normalized radar cross section (NRCS) of a random surface using beam illumination. To find the NRCS, we will need to find the mean value of the scattered field, $\langle \vec{E}_s \rangle$, and the mean-squared scattered field, $\langle \vec{E}_s \cdot \vec{E}_s^* \rangle$, also known as the scattered intensity. Many authors in the past have derived expressions for the radar cross section of a surface assuming a plane wave illumination. Here we take the problem from an assumed source field all the way through to the calculation of the backscattered radar cross section. The source field we will use is an infinite tapered electric field. The radiation by this source field is calculated in Appendix B, using the plane wave spectrum approach.

The derivation of the fields scattered by random surfaces can take two main courses: the first is a Monte Carlo simulation where many realizations of a surface are generated and surface currents on each realization are determined. This approach, though computationally intense, will give exact results. The scattered fields resulting from the various surfaces are averaged to find the expected value of the scattered field. The second approach requires analytical averaging and simplifying assumptions in order to derive a result which is

numerically integrable or can be found in an asymptotic limit. The second approach is the one taken in this thesis. The motivation is to gain insight into the physical aspects of the beam illumination.

Our analysis assumes a source field which when radiated, via the plane wave spectrum approach, yields a Gaussian beam solution as the radiated field. This source distribution has been used in optics to approximate the field in the aperture of a laser [1] and work has been done using multimode Gaussian beam solutions to find the fields radiated by a corrugated horn, where it is shown that the fundamental Gaussian beam solution contains the majority of the radiated power[2]. We will investigate the scattered fields produced when a random perfect electric conductor (PEC) is illuminated by the Gaussian beam. We will check the results to show that they are consistent with the case of a plane wave illuminated random PEC in the proper regimes.

The surface of the random PEC is assumed to comprise Gaussian distributed heights and slopes, both with zero mean. The correlation function is assumed to be Gaussian also. Appendix D gives the functional form of these quantities. By invoking the central limit theorem, which states that if a process is determined by a sum of a large number of independent random variables it yields an overall process which will tend to be Gaussian, we justify that Gaussian surface statistics may be a good approximation to many surfaces generated by the random forces of nature. A discussion of assuming Gaussian statistics and several studies of the statistics of surfaces is given in [3].

Owing to the similarities between Gaussian beam illumination and a Gaussian tapered plane wave illumination, we will present results showing how an "under illuminated" surface reacts with respect to correlation length. The source required to produce a Gaussian tapered plane wave is not presented. However, if an inverse phase is present in the source plane, such as a lensing

operation, one may generate such an incident field.

The following chapters give a new and novel approach in which Kirchhoff theory can be used to understand the physical nature of random surface scattering. Classically, only cutoff plane waves or tapered waves of many correlation lengths in extent have been used to study random surface returns. The beam cases we explore show interesting results for small spot sizes of illumination. The use of the Stochastic Fourier Transform in finding the averaging provides a straightforward way to deal with the expected values and yields expressions with easily distinguishable quantities. Past techniques using integration by parts to perform the expected values, required assuming many correlation lengths of illumination. The Stochastic Fourier Transform method allows us to probe into this region of illumination on the same order as the correlation length of the surface.

Chapter 2

INCIDENT AND SCATTERED FIELD

2.1 Introduction

In much of the literature on random surface scattering, the incident field is assumed to be a plane wave [4,5,6]. However, a more realistic approach would be to consider surface illuminated with a beam wave such as a Gaussian beam. Assuming a source field in the $z=0$ plane such as, $\vec{E}_a = \{A\hat{x} + B\hat{y}\} exp\left[\frac{-(x^2+y^2)}{W^2}\right]$, where W defines the source field radius, (e^{-1} radius in amplitude) a Gaussian beam can be generated. Although infinite in extent, this source distribution does have finite energy and may be an acceptable approximation to some physical apertures such as a laser [1] or a corrugated horn[2]. The field radiated by this source can be determined by the plane wave spectrum approach. A description of the plane wave spectrum approach is given in Appendix A and the specific radiated field for the Gaussian source is derived in Appendix B; its specific form is,

$$\vec{H}_i = H_o \, exp[-jk_o z] \, exp\left[-D\,(x^2+y^2)\right]\left\{-B\,\hat{x} + A\,\hat{y}\right\}, \quad z > 0 \qquad (2.1)$$

where $k_o = \frac{2\pi}{\lambda}$ (λ electromagnetic wavelength of incident field), W is the source beam radius (e^{-1} amplitude radius in $\vec{E}_a$), A and B are arbitrary polarization constants and,

$$D = \frac{k_o^4 W^2 + j2k_o^3 z}{(k_o^2 W^2)^2 + 4k_o^2 z^2},$$

$$H_o = \frac{-k_o^2 W^2}{\eta(k_o^2 W^2 - j2k_o z)}$$

where η is the intrinsic impedance of free space. This field does not satisfy zero

divergence except close to the z-axis and this restriction must be followed.

This field is due to the source a distance z_d above a random surface, with the geometry as shown in Fig. 2.0. This field is taken to be the incident field upon the rough surface. The following relationships provide the transformation from the source coordinates (x, y, z) to rough surface coordinates (x_o, y_o, z_o),

$$x = -x_o,$$
$$y = y_o \mathrm{C}_\theta + \zeta_o \mathrm{S}_\theta,$$
and
$$z = y_o \mathrm{S}_\theta - \zeta_o \mathrm{C}_\theta + z_d, \tag{2.2a}$$

where $\mathrm{C}_\theta = \cos\theta_i$, $\mathrm{S}_\theta = \sin\theta_i$ and $\zeta_o(x_o, y_o)$ is the random surface height at the point (x_o, y_o). The corresponding unit vectors in the surface coordinates are,

$$\hat{x} = -\hat{x}_o,$$
$$\hat{y} = \mathrm{C}_\theta \hat{y}_o + \mathrm{S}_\theta \hat{z}_o,$$
and
$$\hat{z} = \mathrm{S}_\theta \hat{y}_o - \mathrm{C}_\theta \hat{z}_o. \tag{2.2b}$$

The incident field evaluated on the surface is thus:

$$\vec{\mathrm{H}}_i = \mathrm{H}_{o_t} exp\Big[- jk_o(y_o \mathrm{S}_\theta - \zeta_o \mathrm{C}_\theta + z_d) - \mathrm{D}_t(x_o^2 + (y_o \mathrm{C}_\theta + \zeta_o \mathrm{S}_\theta)^2)\Big]\Big\{\mathrm{B}\hat{x}_o + \mathrm{A}(\mathrm{C}_\theta \hat{y}_o + \mathrm{S}_\theta \hat{z}_o)\Big\}.$$

where
$$\mathrm{D}_t = \frac{k_o^4 \mathrm{W}^2 + j2k_o^3(y_o \mathrm{S}_\theta - \zeta_o \mathrm{C}_\theta + z_d)}{(k_o^2 \mathrm{W}^2)^2 + 4k_o^2(y_o \mathrm{S}_\theta - \zeta_o \mathrm{C}_\theta + z_d)^2}$$

and

$$\mathrm{H}_{o_t} = \frac{-k_o^2 \mathrm{W}^2}{\eta(k_o^2 \mathrm{W}^2 - j2k_o(y_o \mathrm{S}_\theta - \zeta_o \mathrm{C}_\theta + z_d))}.$$

This field will be used to find the current density on the PEC in the following sections. It should be observed that $\lim_{\mathrm{W}\to\infty} \mathrm{D}_t = 0$, and $\lim_{\mathrm{W}\to\infty} \mathrm{H}_o = \frac{1}{\eta}$.

Substituting these limiting cases into the incident field, we note that equation (2.1) becomes a plane wave. This is how we will check our results later, i.e. by letting the source distribution become larger and larger to confirm that we can obtain the plane wave NRCS in this limit.

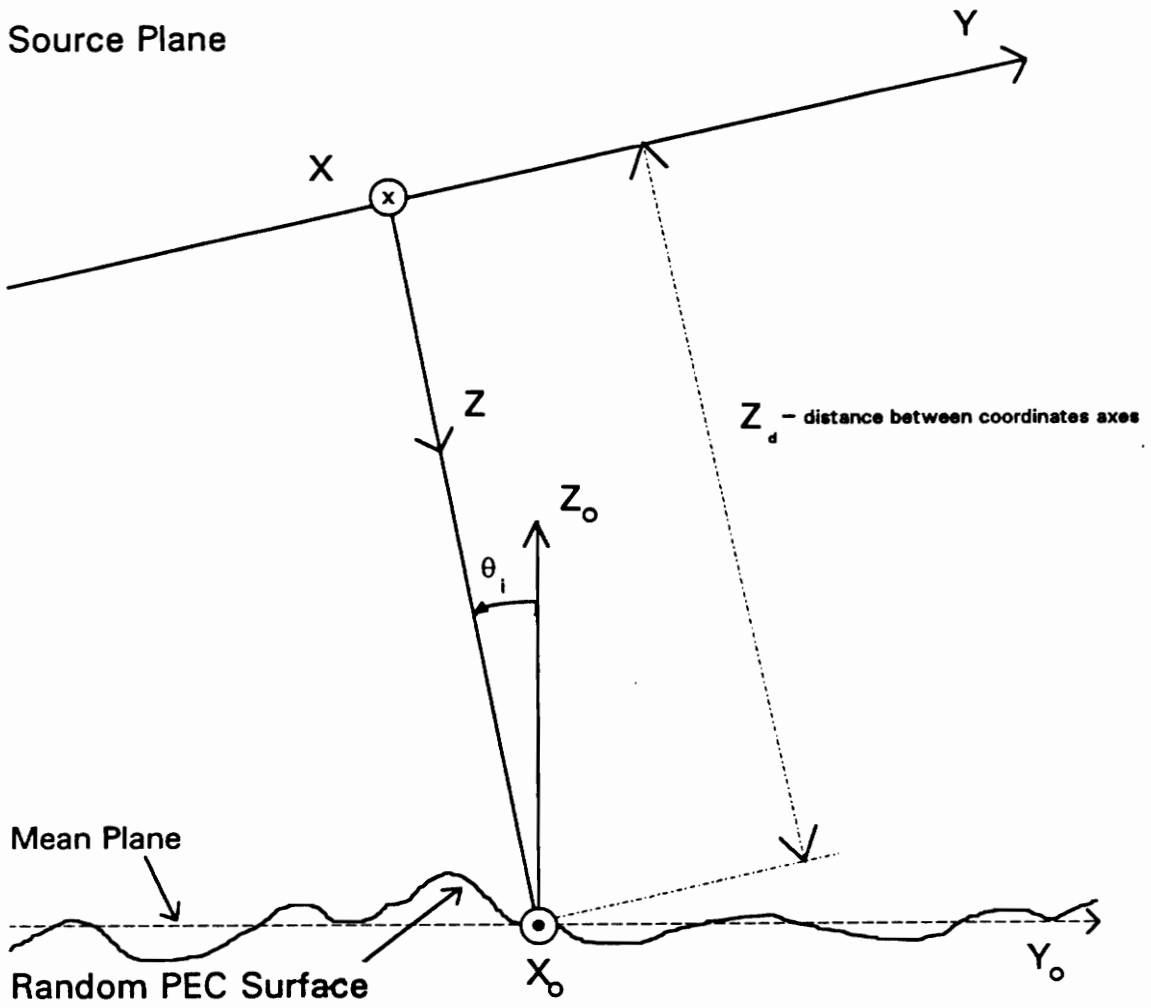

Figure 2.0 Source and Random Surface Geometry.

2.2 Kirchhoff Approximation for Induced Surface Current

If we replace the PEC surface by an equivalent electric surface current, $\vec{J}_s(\vec{r})$, we can calculate the scattered fields[7]. From the boundary conditions on the tangential magnetic field, an integral equation for $\vec{J}_s$ can be formed, e.g.

$$\vec{J}_s = 2\,\hat{n} \times \int_{S_o} \vec{J}_s \times \nabla_o G\, dS_o + 2\,\hat{n} \times \vec{H}_i.$$

The above equation is known as the Magnetic Field Integral Equation (MFIE). Here, $\hat{n}$ is a unit vector normal to the surface as shown in Fig. 2.1, and is defined as

$$\hat{n} = \frac{\left(-\zeta_{x_o}\hat{x}_o - \zeta_{y_o}\hat{y}_o + \hat{z}_o\right)}{|\vec{n}|},$$

where $|\vec{n}| = \sqrt{\zeta_{x_o}^2 + \zeta_{y_o}^2 + 1}$, and $\zeta_{x_o} = \frac{\partial \zeta}{\partial x_o}$, $\zeta_{y_o} = \frac{\partial \zeta}{\partial y_o}$.

The Kirchhoff or Tangent Plane approximation neglects the integral term in the MFIE and simply approximates the current on the surface by $2\,\hat{n} \times \vec{H}_i$. Since this current is exact only when the surface is an infinite flat PEC, we expect that the solution will be valid for surfaces with large radii of curvature and small slopes [3,9,10]. Since the Tangent Plane approximation is a single scatter approximation we expect this result will not hold in near grazing situations. In our work we shall restrict ourselves to 0-10 degrees off normal for both the incident and scattered angles.

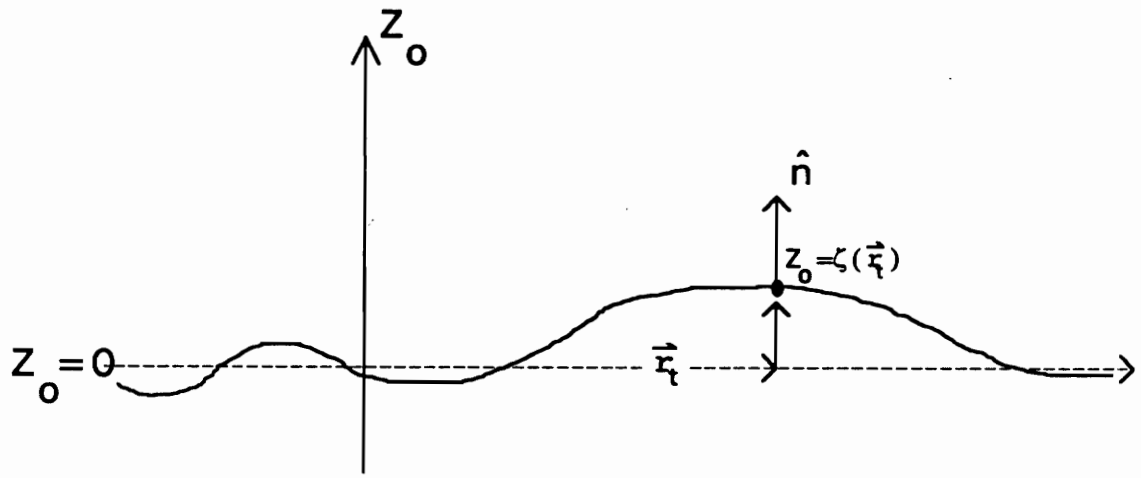

Figure 2.1 Normal to Random Surface.

Using the Tangent Plane approximation the current on the surface is,

$$\vec{J}_s = \frac{2K}{|\vec{n}|}\Big[\ \hat{x}_o\Big\{-\zeta_{y_o}AS_\theta - AC_\theta\Big\} - \hat{y}_o\Big\{-\zeta_{xo}AS_\theta - B\Big\} + \hat{z}_o\Big\{-\zeta_{xo}AC_\theta + \zeta_{yo}B\Big\}\Big],$$

where $K=H_{o_t} exp\Big[-jk_o(y_oS_\theta - \zeta_oC_\theta + z_d) - D_t(x_o^2 + (y_oC_\theta + \zeta_oS_\theta)^2)\Big]$. With this current density, the fields scattered by the random surface can be found. As stated previously, the Kirchhoff current should be used with caution. It neglects multiple scattering and therefore assumes no coupling between currents on the surface. Also, no shadowing by the surface is accounted for. The near normal incidence constraint will greatly reduce shadowing effects.

2.3 Scattered Field via Vector Potential Approach

To find the scattered field we will use the magnetic vector potential approach[8]. To calculate the magnetic vector potential, $\vec{A}$, we only require knowledge of the electric current density on the surface; the electric vector potential, $\vec{F}$, and magnetic current density are zero due to the fact that we are dealing with a PEC surface. By calculating the magnetic vector potential for an impulse current density, we can use superposition to find the magnetic vector potential of an extended current density. The spatial impulse response for free space is the well known Green's Function for free space,

$$G = \frac{exp[-jk_o|\vec{r} - \vec{r}_o|]}{4\pi|\vec{r} - \vec{r}_o|},$$

where $\vec{r}$ is the vector to the observation point, and $\vec{r}_o$ is the vector to each point of current density (source point), see Fig. 2.2.

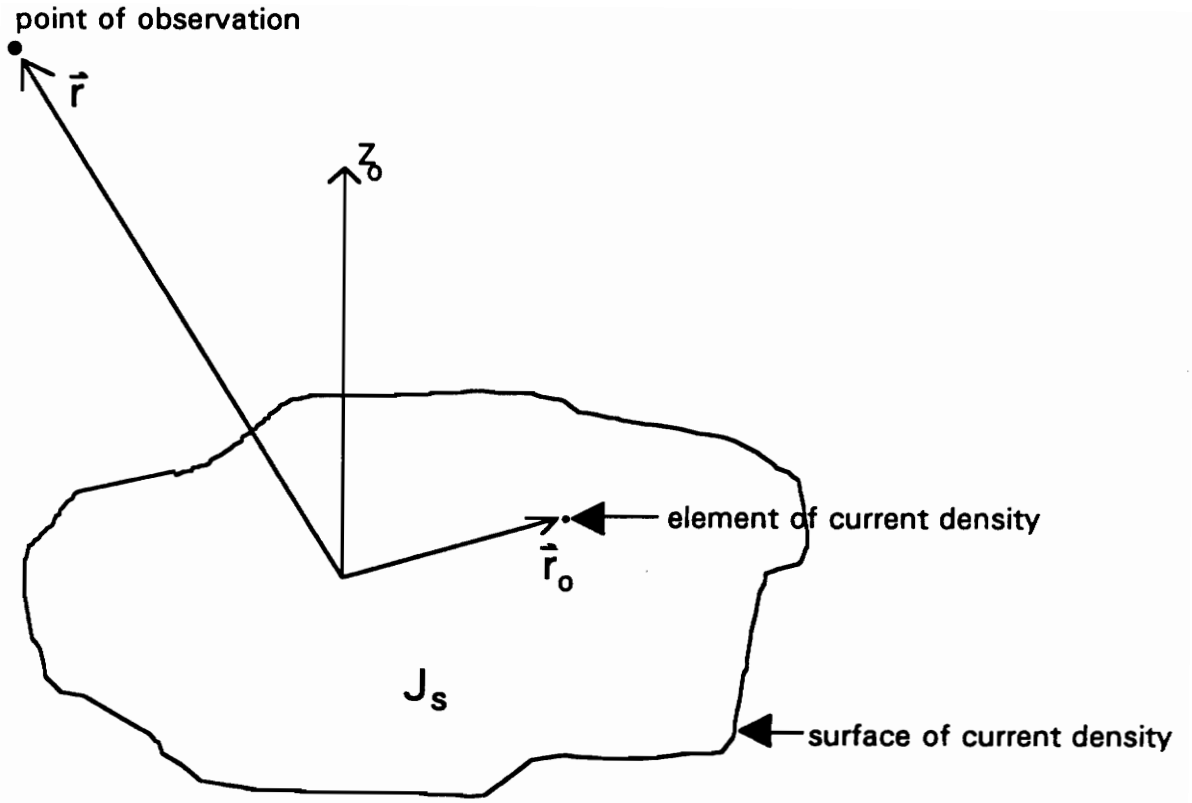

Figure 2.2 Vector Potential Geometry for Integration of the Current Density.

Interpreting the current density as a weighted distribution of point currents, it follows by superposition that,

$$\vec{A} = \int_S \vec{J}_s(\vec{r}) \frac{exp[-jk_o|\vec{r}-\vec{r}_o|]}{4\pi|\vec{r}-\vec{r}_o|} ds_o.$$

The scattered fields outside the source region can then by found from

$$\vec{E}_s = -j\frac{\eta_o}{k_o} \nabla_o \times \nabla_o \times \vec{A}, \tag{2.3}$$

where $k_o = \frac{2\pi}{\lambda}$, and $\eta_o = \sqrt{\frac{\mu_o}{\epsilon_o}}$ (intrinsic impedance of free space). This expression can be simplified by assuming that the ratio of the observation point distance to overall extent of the current density is large. We will consider the scattered field in this limit in the next section.

2.3.1 Fresnel Approximation to Green's Function

By taking our point of observation to be far from the surface, we can simplify equation (2.3) [7]. Taking $\vec{E}_s$ to the "Fresnel zone," we have[7]

$$\vec{E}_s = \frac{jk_o\eta}{4\pi r_r} exp[-jk_o r_r] \hat{k}_s \times (\hat{k}_s \times \int_{S_o} \vec{J}_s \, exp\left[jk_o \hat{k}_s \cdot \vec{r}_o - \frac{jk_o r_o^2}{2r_r}\right] ds_o), \tag{2.4}$$

where r_r is the distance to receiver, $r_o^2 = x_o^2 + y_o^2 + \zeta_o^2$ and $\hat{k}_s$ is the scattered direction, see Fig. 2.3. The distinction between equation (2.4), or the "Fresnel zone" form, and the well known far field form for the scattered field is that we have retained the quadratic phase term in the expansion of the Green's Function exponential. By keeping the quadratic phase term we should be able to obtain solutions with a reduced constraint on the distance r_r, or bring solutions into the Fresnel zone. In Appendix B, we perform a derivation of flat PEC reflection of

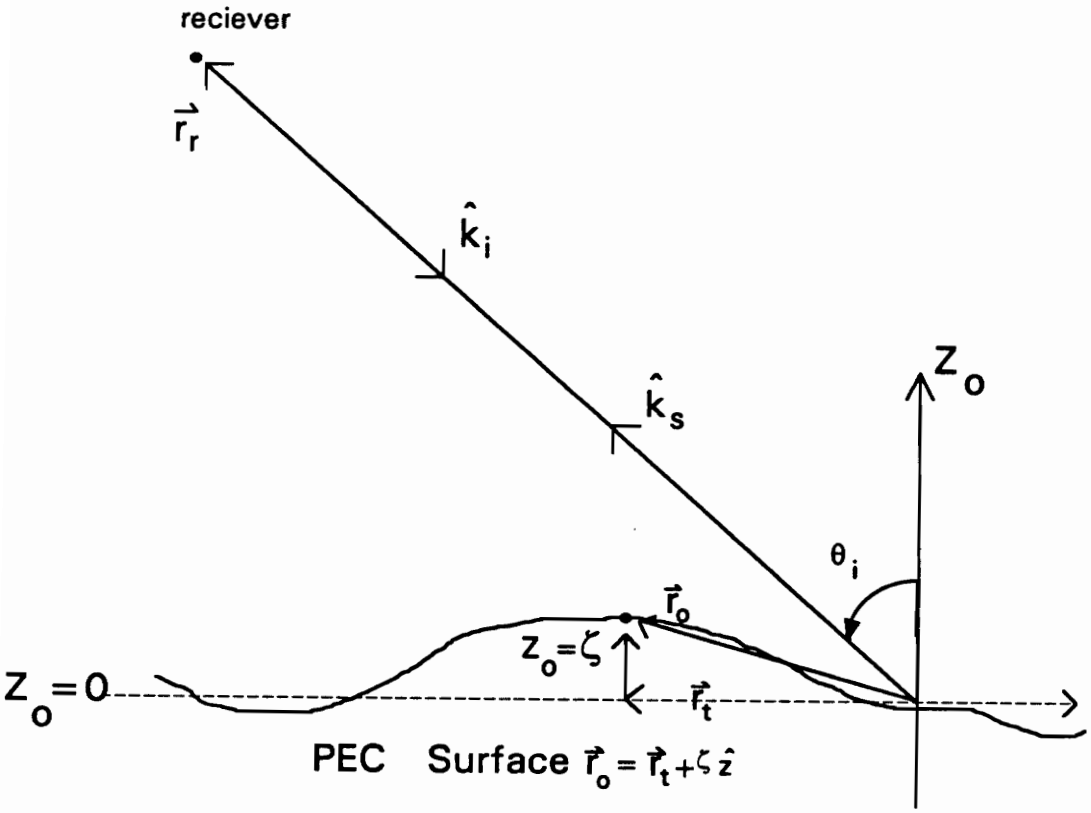

Figure 2.3 Random Surface Integration Geometry.

the incident field where the observation point is co-located with source. It is shown that to find the image theory result, the quadratic phase term must be kept. However, our analysis will be done in the backscattered direction as r_r is large and we therefore neglect it.

As was stated in the introduction, $\langle \vec{E}_s \rangle$ and $\langle \vec{E}_s \cdot \vec{E}_s^* \rangle$ are the field moments we are interested in since they are required to calculate the NRCS. Integration is performed in the z_o=0 plane by projecting each elemental area ds_o to the plane below; this projection results in $ds_o = \sqrt{1+\zeta_{x_o}{}^2+\zeta_{y_o}{}^2}\, dx_o dy_o$ and thus,

$$\vec{E}_s = \frac{jk_o\eta}{2\pi r_r} exp[-jk_o r_r]\, \hat{k}_s \times (\, \hat{k}_s \times \int_{-\infty}^{\infty} \int_{-\infty}^{\infty} \Big[-\hat{x}_o \Big\{ \zeta_{y_o} \mathrm{AS}_\theta + \mathrm{AC}_\theta \Big\} + \hat{y}_o \Big\{ \zeta_{xo} \mathrm{AS}_\theta + \mathrm{B} \Big\}$$

$$+ \hat{z}_o \Big\{ -\zeta_{xo} \mathrm{AC}_\theta + \zeta_{yo} \mathrm{B} \Big\} \Big]\, \mathrm{K}\, exp\Big[jk_o \hat{k}_s \cdot \vec{r}_o - \frac{jk_o r_o^2}{2r_r} \Big] dx_o dy_o.$$

with $\hat{k}_s \cdot \vec{r}_o = x_o \sin\theta\cos\phi + y_o \sin\theta\sin\phi + \zeta_o \cos\theta$. The angles θ and ϕ are shown in Fig. 2.4. The above expression contains the following random variables; random height ζ_o, and random slopes in the x and y directions, ζ_{xo} and ζ_{y_o} respectively. The quadratic phase term is still present in the above equation, and we will keep it throughout the derivation. It will be entered as a very large number during numerical calculation and the quadratic phase term divided by r_r is negligible. In the next section we will simplify this expression to the backscatter direction.

2.3.2 Backscattered Field

In order to reduce the complexity of the averaging, we will consider only the case of backscatter in this thesis. This is done because for the underlying motivation of this thesis, namely surface characteristic determination, the backscatter case is of the most practical interest. First we will recall the incident

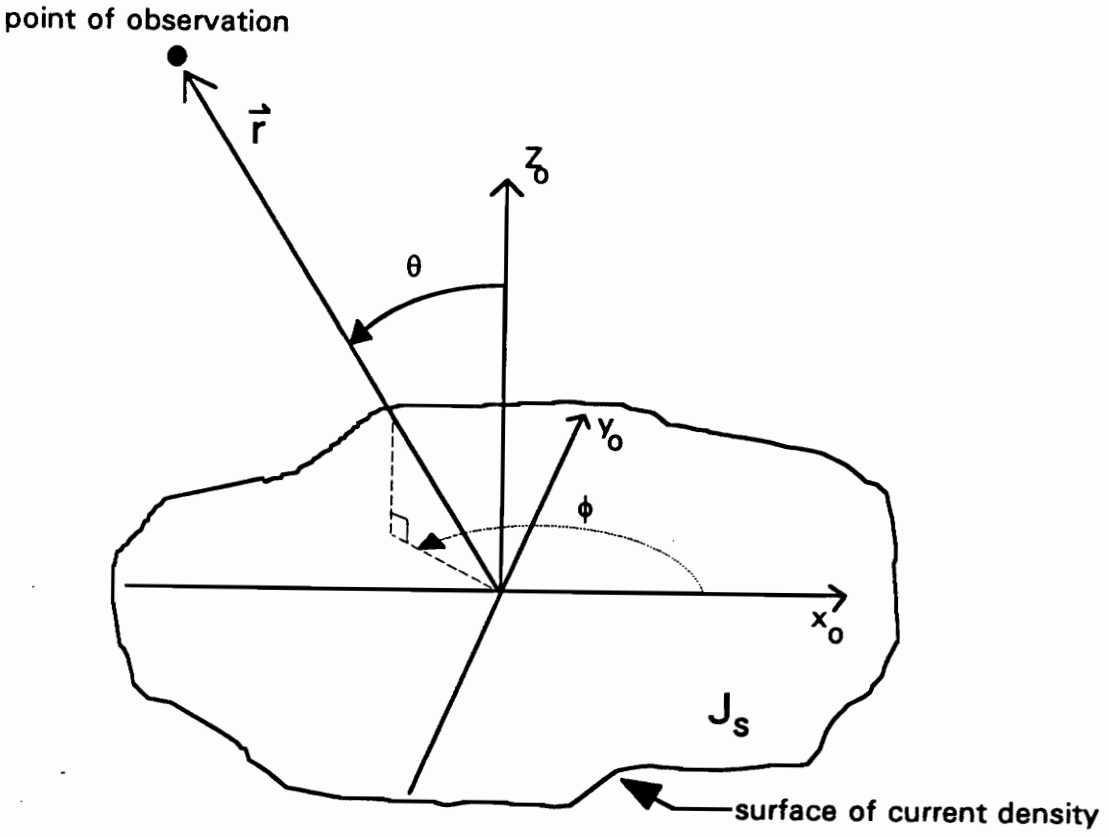

Figure 2.4 General Scattering Surface Geometry.

wave vector, $\hat{k}_i$, (referring back to the coordinate transformations eqs. (2.2a-b)) can be seen to be equal to the transformed source vector $\hat{z}$. Therefore, $\hat{k}_i = S_\theta \hat{y}_o - C_\theta \hat{z}_o$ in PEC surface coordinates. For backscatter, the scattering direction, $\hat{k}_s$, will equal -$\hat{k}_i$. Therefore, $\hat{k}_s = S_\theta \hat{y}_o - C_\theta \hat{z}_o$ and the resulting equation for $\vec{E}_s$ becomes

$$\vec{E}_s = \frac{-jk_o\eta}{2\pi r_r} exp[-jk_o r_r] \int_{-\infty}^{\infty} \int_{-\infty}^{\infty} \Big\{ -\hat{x}_o(\zeta_{y_o} AS_\theta + AC_\theta) + \hat{y}_o(C_\theta S_\theta \zeta_{y_o} B + BC_\theta^2)$$

$$+ \hat{z}_o(BS_\theta^2 \zeta_{y_o} + BS_\theta C_\theta) \Big\} H_{o_t} exp\Big[-jk_o(y_o S_\theta - \zeta_o C_\theta + z_d)\Big]$$

$$exp\Big[-D_t\Big(x_o^2 + (y_o C_\theta + \zeta_o S_\theta)^2\Big)\Big] exp\left[jk_o \hat{k}_s \cdot \vec{r}_o - \frac{jk_o r_o^2}{2r_r}\right] dx_o dy_o. \qquad (2.5)$$

The choice of incident direction and backscatter has reduced the number of random variables we must average over to the random height ζ_o and the random slope in the y direction ζ_{y_o}. The loss of the slope in the x direction is a result of our incident geometry and the fact that the Kirchhoff approximation does not preserve cross polarization affects due to multiple bounces.

Chapter 3

MEAN SCATTERED FIELD

3.1 Motivation

In order to find the NRCS, which is defined as;

$$\sigma^o = \lim_{r_r \to \infty} \frac{4\pi {r_r}^2 \left(\langle \vec{E}_s \cdot \vec{E}^*_s \rangle - \langle \vec{E}_s \rangle \cdot \langle \vec{E}^*_s \rangle \right)}{\int_{-\infty}^{\infty} \int_{-\infty}^{\infty} | E_i |^2 ds_o}. \tag{3.1}$$

we will need to take the expected value of $\vec{E}_s$ and also its intensity. Appendix F contains a brief discussion of the considerations for the NRCS. The NRCS, which is utilized in the radar equation, is a measure of the surface scattering cross section (in a certain direction) per unit scattering area of surface. The total power incident upon the surface is given by $\int_{-\infty}^{\infty} \int_{-\infty}^{\infty} | E_i |^2 ds_o$, where ds_o is taken over the mean surface. This is often shown as $A_{ill} E_o^2$ when a finite surface is illuminated by a plane wave. Since we are using an infinite surface and a more complicated form for the incident field, we need a more general normalization.

The quantities in the numerator $4\pi {r_r}^2$, $\langle \vec{E}_s \cdot \vec{E}^*_s \rangle$, and $\langle \vec{E}_s \rangle \cdot \langle \vec{E}^*_s \rangle$ represent the spherical propagation spreading, total power scattered and coherent power scattered, respectively. The spherical propagation spreading is already contained in the radar equation and must therefore be removed from $\langle \vec{E}_s \cdot \vec{E}^*_s \rangle$ and $\langle \vec{E}_s \rangle \cdot \langle \vec{E}^*_s \rangle$ by multiplication of the $4\pi {r_r}^2$ factor. Calculation of the total and coherent scattered power are the objectives of the remainder of this thesis. We will begin with the easier of the two quantities, the coherent scattered power.

The expected value of the scattered field, $\langle \vec{E}_s \rangle$, can be shown explicitly by introducing the probability density function for the random variables as,

$$\langle \vec{E}_s \rangle = \frac{-jk_o\eta}{2\pi r_r} exp[-jk_o r_r] \int_{-\infty}^{\infty} \int_{-\infty}^{\infty} \int_{-\infty}^{\infty} \Big\{ -\hat{x}_o(\zeta_{y_o} AS_\theta + AC_\theta) + \hat{y}_o(C_\theta S_\theta \zeta_{y_o} B + BC_\theta^2)$$

$$+ \hat{z}_o(S_\theta^2 \zeta_{y_o} A + BS_\theta C_\theta) \Big\} H_{o_t} exp\Big[-jk_o(y_o S_\theta - \zeta_o C_\theta + z_d)\Big]$$

$$\cdot exp\Big[-D_t\Big(x_o^2 + (y_o C_\theta + \zeta_o S_\theta)^2\Big)\Big] exp\left[jk_o \hat{k}_s \cdot \vec{r}_o - \frac{jk_o r_o^2}{2r_r}\right]$$

$$\cdot \mathrm{pdf}(\zeta_o, \zeta_{y_o}) dx_o dy_o,$$

where $\mathrm{pdf}(\zeta_o, \zeta_{y_o})$ is the probability density function for a single point height and slope. A description of the surface statistics to be used are given in Appendix D. Since the height and slope at a single point are independent, we can write $\mathrm{pdf}(\zeta_o, \zeta_{y_o}) = \mathrm{pdf}(\zeta_o)\mathrm{Pdf}(\zeta_{y_o})$. Performing the integration over the slope yields

$$\langle \vec{E}_s \rangle = \frac{-jk_o\eta H_o}{2\pi r_r} exp\Big[-jk_o(r_r + z_d)\Big] \Big\{ -\hat{x}_o AC_\theta + \hat{y}_o BC_\theta^2 + \hat{z}_o BS_\theta C_\theta \Big\} \tag{3.2}$$

$$\int_{-\infty}^{\infty} \cdots \int_{-\infty}^{\infty} exp[-jk_o(y_o S_\theta - \zeta_o C_\theta)] exp\Big[-D_t\Big(x_o^2 + (y_o C_\theta + \zeta_o S_\theta)^2\Big)\Big] exp[jk_o(-S_\theta y_o + C_\theta \zeta_o)]$$

$$exp\left[-jk_o \frac{x_o^2 + y_o^2 + \zeta_o^2}{2r_r}\right] \mathrm{Pdf}(\zeta_o) d\zeta_o \, dx_o dy_o,$$

where zero mean slopes have been assumed. Given that the observation point r_r is tending to infinity we will neglect the quadratic dependence on the random height since this term tends to zero. An attempt to keep this quadratic dependence on the random height can be completed by expanding out the probability density functions for the heights and lumping the quadratic terms

from the pdf together with other quadratic height terms in the integrand. However, the completion of the averaging for $\langle | \vec{E}_s |^2 \rangle$ becomes too intractable to complete when we keep the quadratic height. Several attempts at expanding the two point pdf's used in the calculation of $\langle | \vec{E}_s |^2 \rangle$ and lumping the quadratic heights in the expression were tried, but failed to lead to anything tractable.

3.2 Near Normal Incidence Approximation to Taper

Looking at equation (3.2) we note that the surface transformations have also introduced quadratic random height terms in the exponentials. Since we are concerned with near normal incidence in the backscatter direction and far from the surface $S_\theta \approx 0$ and $z_d \gg \zeta_o$. Therefore, we can make the following approximations:

$$exp\Big[- D_t(x_o^2 + (y_o C_\theta + \zeta_o S_\theta)^2) \Big] \approx exp\left[- \frac{k_o^4 W^2 + j2k_o^3 z_d}{(k_o^2 W^2)^2 + 4k_o^2 z_d^2} \ (x^2{}_o + y_o^2 C_\theta^2) \right] \tag{3.3}$$

and

$$H_{o_t} \approx \frac{-k_o^2 W^2}{\eta(k_o^2 W^2 - j2k_o z_d)}. \tag{3.4}$$

Assuming a Gaussian pdf for the heights and grouping the terms with random heights together yields

$$\langle \vec{E}_s \rangle = \frac{-jk_o \eta H_{o_t}}{2\pi r_r} exp\Big[- jk_o(r_r + z_d) \Big] \Big\{ - \hat{x}_o A C_\theta + \hat{y}_o B C_\theta{}^2 + \hat{z}_o B S_\theta C_\theta \Big\}$$

$$\int_{-\infty}^{\infty} \int_{-\infty}^{\infty} \left(\int_{-\infty}^{\infty} \frac{1}{\sqrt{2\pi \langle \zeta_o^2 \rangle}} exp\left[- \frac{\zeta_o{}^2}{2\langle \zeta_o^2 \rangle} \right] exp[j\zeta_o (k_o 2C_\theta)] \, d\zeta_o \right)$$

$$exp\Big[- (D_x x_o^2 + D_y y_o^2) \Big] exp[- jk_o 2S_\theta y_o] dx_o dy_o,$$

where

$$D_x = \frac{k_o^4 W^2 + j2k_o^3 z_d}{(k_o^2 W^2)^2 + 4k_o^2 z_d^2} + \frac{jk_o}{2r_r} \quad \text{and} \quad D_y = C_\theta^2 \frac{k_o^4 W^2 + j2k_o^3 z_d}{(k_o^2 W^2)^2 + 4k_o^2 z_d^2} + \frac{jk_o}{2r_r}.$$

The integration in parenthesis is simply the Fourier transform of the Gaussian pdf, also known as the characteristic function $\Phi(k_o 2C_\theta) = exp\left[-2k_o^2 C_\theta{}^2 \langle \zeta_o^2 \rangle\right]$. Performing the integration yields

$$\langle \vec{E}_s \rangle = \frac{-jk_o \eta H_{o_t}}{2\pi r_r} exp\left[-jk_o(r_r + z_d)\right] \left\{ -\hat{x}_o AC_\theta + \hat{y}_o BC_\theta{}^2 + \hat{z}_o BS_\theta C_\theta \right\}$$

$$\int_{-\infty}^{\infty} \int_{-\infty}^{\infty} \Phi(k_o 2C_\theta) exp\left[-(D_x x_o^2 + D_y y_o^2)\right] exp\left[-jk_o 2S_\theta y_o\right] dx_o dy_o. \qquad (3.5)$$

Before going forward with the remaining surface integrations, $dx_o dy_o$, we should note some of the characteristics of equation (3.5). First, it has no dependence on the random surface's correlation length. For the surface statistics we assumed, the variance of the heights $\langle \zeta_o^2 \rangle$ and the correlation length l^2 are the only parameters needed to describe the surface. One would expect the average scattered field to be a function of both of these parameters. The dependence only on the variance of the heights is sometimes called the "elevated plane" result, due to the fact that the solution looks as if it resulted from reflection by a randomly undulating plane[11]. This is a result of the Kirchhoff or tangent plane approximation to the equivalent currents set up by the incident field.

3.3 Average Coherent Power

Next, we will complete the surface integrations of equation (3.5) and form the coherent power. Using the useful integral form, $\int_{-\infty}^{\infty} exp\left[-at^2 + bt\right] dt = \sqrt{\frac{\pi}{a}}\, exp\left[\frac{b^2}{4a}\right]$, Re(a>0), [12] we can evaluate the two integrals, resulting in (Re[D_x] and

$\mathrm{Re}[D_y]>0$)

$$\langle \vec{E}_s \rangle = \frac{-jk_o\eta H_{o_t}}{2\pi r_r} exp\left[-jk_o(r_r+z_d)\right] exp\left[-2k_o^2 C_\theta^{\,2}\langle\zeta_o^2\rangle\right] exp\left[-\frac{k_o^2}{D_y} S_\theta^2\right]$$

$$\frac{\pi}{\sqrt{D_y D_x}} \left\{-\hat{x}_o A C_\theta + \hat{y}_o B C_\theta^{\,2} + \hat{z}_o B S_\theta C_\theta\right\}. \tag{3.6}$$

The coherent power is thus given by

$$\langle \vec{E}_s \rangle \cdot \langle \vec{E}_s^{\,*} \rangle = \left(\frac{k_o\eta\,|H_{o_t}|}{2\pi r_r}\right)^2 C_\theta^{\,2}\, exp\left[-4k_o^2 C_\theta^{\,2}\langle\zeta_o^2\rangle\right] exp\left[-k_o^2 S_\theta^2 \frac{2\mathrm{Re}[D_y]}{|D_y|^2}\right]$$

$$\cdot \frac{\pi^2}{|D_x||D_y|}(A^2+B^2), \tag{3.7}$$

where $H_{o_t} = \dfrac{-k_o^2 W^2}{\eta(k_o^2 W^2 - j2k_o z_d)}$, $D_x = \dfrac{k_o^4 W^2 + j2k_o^3 z_d}{(k_o^2 W^2)^2 + 4k_o^2 z_d^2} + \dfrac{jk_o}{2r_r}$

and $D_y = C_\theta^2 \dfrac{k_o^4 W^2 + j2k_o^3 z_d}{(k_o^2 W^2)^2 + 4k_o^2 z_d^2} + \dfrac{jk_o}{2r_r}$.

Several authors,[3],[6],[13], have shown that in the Kirchhoff approximation the coherent field is simply the flat plane reflected field attenuated due to the roughness. If we expand out equation (3.7), we would see that as $W\to\infty$ the expression becomes proportional to $W^4 exp(-k_o^2 S_\theta^2 W^2)$. The exponential will dominate the coherent power and produce zero except when $S_\theta^2 = 0$. This is quite correct; a plane wave incident ($W\to\infty$) will reflect only in the specular direction. When the backscatter and specular directions are the same (normal incidence), the S_θ^2 term will be zero giving a coherent field. Since in this thesis W will not be evaluated for $W = \infty$, we see that we will get coherent power in the backscatter direction for angles other than normal incidence. This is due to the

spreading of the incident Gaussian beam. The coherent power will be small, however, due to the rms surface heights we will use, and that we are in backscatter.

Chapter 4

MEAN SQUARED BACKSCATTERED FIELD

4.1 Introduction

Equation (2.5) for the scattered electric field, shown below, will be used to find the mean squared backscattered field, or total power:

$$\vec{E}_s=\frac{-jk_o\eta}{2\pi r_r}exp[-jk_o r_r]\int_{-\infty}^{\infty}\int_{-\infty}^{\infty}\Big\{-\hat{x}_o(\zeta_{y_o}AS_\theta+AC_\theta)+\hat{y}_o(C_\theta S_\theta\zeta_{y_o}B+BC_\theta{}^2)$$

$$+\hat{z}_o(S_\theta{}^2\zeta_{y_o}+BS_\theta C_\theta)\Big\}\,H_{o_t}exp\Big[-jk_o(y_oS_\theta-\zeta_oC_\theta+z_d)\Big]$$

$$exp\Big[-D_t\Big(x_o^2+(yC_\theta+\zeta_oS_\theta)^2\Big)\Big]exp\left[jk_o\hat{k}_s\cdot\vec{r}_o-\frac{jk_or_o^2}{2r_r}\right]dx_o dy_o. \qquad (4.1)$$

As was done in the calculation of the average field, $S_\theta \approx 0$, and, therefore, the $\zeta_o S_\theta$ term will be dropped in the exponential. The quadratic taper and phase factor will also be approximated as in equations (3.3) and (3.4). The mean squared backscattered field will be calculated by forming $\langle \vec{E}_s \cdot \vec{E}_s{}^* \rangle$, or

$$\langle \vec{E}_s \cdot \vec{E}_s{}^* \rangle = \left\langle \left(\frac{k_o\eta\,|H_{o_t}|}{2\pi r_r}\right)^2 \int_{-\infty}^{\infty}\cdots\int_{-\infty}^{\infty}\Big\{(\zeta_{y_o}AS_\theta+AC_\theta)(\zeta_{y_1}AS_\theta+AC_\theta)\right.$$

$$+(C_\theta S_\theta\zeta_{y_o}B+BC_\theta{}^2)(C_\theta S_\theta\zeta_{y1}B+BC_\theta{}^2)$$

$$+(S_\theta{}^2\zeta_{y_o}+BS_\theta C_\theta)(S_\theta{}^2\zeta_{y1}+BS_\theta C_\theta)\Big\}$$

$$exp\Big[-jk_o(2S_\theta(y_o-y_1)-2C_\theta(\zeta_o-\zeta_1)\Big]$$

$$\left. exp\Big[-(D_x x_o^2+D_y y_o^2)-(D_x{}^* x_1^2+D_y{}^* y_1^2)\Big]dx_o dy_o dx_1 dy_1\right\rangle.$$

Simplifying this expression yields the form

$$\langle \vec{E}_s \cdot \vec{E}_s^{\,*} \rangle = Q \left\langle \int_{-\infty}^{\infty} \cdots \int_{-\infty}^{\infty} \left\{ S_\theta^{\,2}\, \zeta_{yo}\zeta_{y1} + C_\theta S_\theta (\zeta_{yo} + \zeta_{y1}) + C_\theta^{\,2} \right\} \right.$$

$$exp\left[jk_o 2C_\theta(\zeta_o - \zeta_1) - jk_o 2S_\theta(y_o - y_1) \right]$$

$$\left. exp\left[-(D_x x_o^2 + D_y y_o^2) - (D_x^{\,*} x_1^2 + D_y^{\,*} y_1^2) \right] dx_o dy_o dx_1 dy_1 \right\rangle, \qquad (4.2)$$

where $Q = \left(\frac{k_o \eta \, |H_{o_t}|}{2\pi r_r} \right)^2 (A^2 + B^2)$.

Inspecting equation (4.2), it is noted that for the specific case of backscatter, the required pdf is pdf(ζ_{yo},ζ_{y1},ζ_o,ζ_1). Performing this averaging has been done by several authors [3,6,13] when the taper function is real valued. Generally they use integration by parts which gives rise to "edge effects" for finitely illuminated surfaces. These "edge effects" can lead to difficulties if not dealt with properly. However, there is another method which can be used owing to the fact that we have assumed Gaussian statistics. It utilizes the Stochastic Fourier Transform[14]. For the case of plane wave illumination and using both numerical and asymptotic evaluations, we have numerically compared these two methods and they do agree.

4.2 Averaging via Stochastic Fourier Transform Method

In this section we will discuss how the averaging required for equation (4.2) can be found using the Stochastic Fourier Transform method [14]. We introduce dummy Fourier transform variables k_2 and k_3 corresponding to the ζ_{y1} and ζ_{yo} slope variables, respectively. We also define another variable k_z=k_o2C$_\theta$, and then consider the following expected value of the slope product term, i.e.

$$\left\langle \zeta_{y1}\zeta_{yo} exp[j(k_z\zeta_o + (-k_z)\zeta_1)] \right\rangle = \int_{-\infty}^{\infty} \cdots \int_{-\infty}^{\infty} \zeta_{y1}\zeta_{yo} \mathrm{Pdf}(\zeta_o,\zeta_1,\zeta_{yo},\zeta_{y1})$$

$$exp\Big[j(k_2\zeta_{y1} + k_3\zeta_{yo} + k_z\zeta_o + (-k_z)\zeta_1)\Big] d\zeta_o d\zeta_1 d\zeta_{yo} d\zeta_{y1} \Big|_{k_2 = k_3 = 0}.$$

The above integrals simplify to

$$\left\langle \zeta_{y1}\zeta_{yo} exp[j(k_z\zeta_o + (-k_z)\zeta_1)] \right\rangle = \left[-\frac{\partial^2}{\partial k_2 \partial k_3} \mathfrak{F}\{\mathrm{Pdf}(\zeta_o,\zeta_1,\zeta_{yo},\zeta_{y1})\} \right]_{k_2 = k_3 = 0},$$

where $\mathfrak{F}\{\}$ is the Fourier transform of the pdf over all the random variables. The characteristic function for a multivariate Gaussian pdf with all random variables zero mean is [15],

$$\Psi_x(\omega_1,\omega_2,...,\omega_n) = exp\Big[-\tfrac{1}{2}\,\boldsymbol{\omega}^{\mathbf{T}} \boldsymbol{\Sigma}_{\boldsymbol{x}} \boldsymbol{\omega}\Big].$$

where $\boldsymbol{\omega}^{\mathbf{T}} = (\omega_1,\omega_2,...,\omega_n)$, $\boldsymbol{\Sigma}_{\boldsymbol{x}}$ is the covariance matrix, and $\boldsymbol{\omega}$ is a column matrix of ω_i. After some algebra and differentiation, the result for the expected values is given as,

$$\left\langle \zeta_{y1}\zeta_{yo} exp[j(k_z\zeta_o + (-k_z)\zeta_1)] \right\rangle = -\left\{ \mathrm{R}_{yy} + k_o^2 4\mathrm{C}_\theta{}^2 \mathrm{R}_y{}^2 \right\} exp\Big[-k_o^2 4\mathrm{C}_\theta{}^2 (\langle \zeta_o^2 \rangle - \mathrm{R}) \Big],$$

where the autocorrelation function R and its derivatives are given by

$$R = \langle \zeta_o^2 \rangle exp\left[-\frac{(\Delta x^2 + \Delta y^2)}{l^2} \right],$$

$$R_y = \frac{\partial R}{\partial \Delta y} = -\frac{2\,\langle \zeta_o^2 \rangle}{l^2}\,\Delta y\; exp\left[-\frac{(\Delta x^2 + \Delta y^2)}{l^2} \right],$$

and

$$R_{yy} = \frac{\partial^2 R}{\partial \Delta y^2} = -\frac{2\,\langle \zeta_o^2 \rangle}{l^2}\left(1 - \frac{2\Delta y^2}{l^2} \right) exp\left[-\frac{(\Delta x^2 + \Delta y^2)}{l^2} \right].$$

Using the same method as above, the single slope and two heights expected values are obtained; specifically,

$$\left\langle \zeta_{yo} exp[j(k_z \zeta_o + (-k_z)\zeta_1)] \right\rangle = -jk_o 2C_\theta R_y exp\left[-k_o^2 4C_\theta{}^2 (\langle \zeta_o^2 \rangle - R) \right],$$

$$\left\langle \zeta_{y1} exp[j(k_z \zeta_o + (-k_z)\zeta_1)] \right\rangle = -jk_o 2C_\theta R_y exp\left[-k_o^2 4C_\theta{}^2 (\langle \zeta_o^2 \rangle - R) \right],$$

and

$$\left\langle exp[j(k_z \zeta_o + (-k_z)\zeta_1)] \right\rangle = exp\left[-k_o^2 4C_\theta{}^2 (\langle \zeta_o^2 \rangle - R) \right].$$

The final result for the average backscattered power then becomes

$$\langle \vec{E}_s \cdot \vec{E}_s^* \rangle = Q \int_{-\infty}^{\infty} \int_{-\infty}^{\infty} \left\{ -(R_{yy} + R_y{}^2 k_o^2 4C_\theta{}^2) S_\theta{}^2 - j4R_y k_o C_\theta{}^2 S_\theta + C_\theta{}^2 \right\}$$

$$exp\left[-k_o^2 4C_\theta{}^2 (\langle \zeta_o^2 \rangle - R) \right] exp\left[-jk_o 2S_\theta (y_o - y_1) \right]$$

$$exp\left[-(D_x x_o^2 + D_y y_o^2) - (D_x{}^* x_1^2 + D_y{}^* y_1^2) \right] dx_o dy_o dx_1 dy_1.$$

Converting this into $\Delta x = x_o - x_1$, $\Delta y = y_o - y_1$, x_o, and y_o coordinates yields,

$$\langle \vec{E}_s \cdot \vec{E}_s^* \rangle = Q \int_{-\infty}^{\infty} \cdots \int_{-\infty}^{\infty} \left\{ -(R_{yy} + R_y{}^2 k_o^2 4 C_\theta{}^2) S_\theta{}^2 - j4 R_y k_o C_\theta{}^2 S_\theta + C_\theta{}^2 \right\}$$

$$exp\left[-2\mathrm{Re}[D_x]\ x_o^2 + D_x{}^* 2\Delta x\ x_o - 2\mathrm{Re}[D_y]\ y_o^2 + D_y{}^* 2\Delta y\ y_o\right]$$

$$exp\left[-(D_x{}^* \Delta x^2 + D_y{}^* \Delta y^2) \right] exp\left[-jk2S_\theta \Delta y \right]$$

$$exp\left[-k_o^2 4 C_\theta{}^2 (\langle \zeta_o^2 \rangle - R) \right] dx_o dy_o d\Delta x d\Delta y.$$

Integrating the x_o and y_o variables, results in the expression

$$\langle \vec{E}_s \cdot \vec{E}_s{}^* \rangle = Q \int_{-\infty}^{\infty} \cdots \int_{-\infty}^{\infty} \left\{ -(R_{yy} + R_y{}^2 k_o^2 4 C_\theta{}^2) S_\theta{}^2 - j4 R_y k_o C_\theta{}^2 S_\theta + C_\theta{}^2 \right\}$$

$$\frac{\pi}{2\sqrt{\mathrm{Re}[D_x]\mathrm{Re}[D_y]}}\ exp\left[\left(\frac{(D_x{}^*)^2}{2\mathrm{Re}[D_x]} \Delta x^2 + \frac{(D_y{}^*)^2}{2\mathrm{Re}[D_y]} \Delta y^2 \right) \right]$$

$$exp\left[-(D_x{}^* \Delta x^2 + D_y{}^* \Delta y^2) \right] exp\left[-jk2S_\theta \Delta y \right]$$

$$exp\left[-k_o^2 4 C_\theta{}^2 (\langle \zeta_o^2 \rangle - R) \right] d\Delta x d\Delta y. \tag{4.3}$$

Although $\langle \vec{E}_s \cdot \vec{E}_s{}^* \rangle$ must be real, it may not be obvious by a simple inspection of equation (4.3). However, since R_{yy} and R_y are even and odd functions respectively, the above expression simplifies to,

$$\langle \vec{E}_s \cdot \vec{E}_s^{*} \rangle = Q \frac{\pi}{2\mathrm{Re}[D_x]\, C_\theta} \int_{-\infty}^{\infty}\int_{-\infty}^{\infty} \Big\{ \Big[-(R_{yy} + R_y{}^2 k_o^2 4 C_\theta{}^2) S_\theta{}^2 + C_\theta{}^2 \Big] cos(k_o 2 S_\theta \Delta y)$$

$$- 4 R_y k_o C_\theta{}^2 S_\theta sin(k_o 2 S_\theta \Delta y) \Big\}$$

$$exp\left[-\left(\frac{|D_x|^2}{2\mathrm{Re}[D_x]} \right) \Delta x^2 \right] exp\left[-\left(\frac{|D_y|^2}{2\mathrm{Re}[D_y]} \right) \Delta y^2 \right]$$

$$exp\Big[-k_o^2 4 C_\theta{}^2 (\langle \zeta_o^2 \rangle - R) \Big] d\Delta x d\Delta y, \qquad (4.4)$$

which is non-negative real.

It should be stated that one can obtain equation (4.3) using Bayes theorem. However, the method is quite cumbersome algebraically. It does indeed give the same result, however.

In the next section we will examine (4.3) under approximations to the Δx and the Δy integrals. Equation (4.3) shows the explicit dependence on the autocorrelation function in the multiplier term as well as in the exponential. Seeing these terms and having an intuitive feel for their functional dependence can help one gain physical insight into the process of random surface scattering. For example, it should be noted that as we make the correlation length tend to infinity, meaning that the surface is actually an undulating plane, both R_{yy} and R_y are zero, resulting in a solution which is the same as that in equation (3.7) for the average coherent power.

4.3 Asymptotic Solution

Examining equation (4.3), we note that the exponential term containing R is the impediment to further analytic integration. This term may be approximated for certain conditions (namely $k_o^2 4 C_\theta{}^2 \langle \zeta_o^2 \rangle$ large) to yield an approximate integration [3,6,13]. The approximate result is

$$exp\Big[-k_o^2 4C_\theta{}^2(\langle\zeta_o^2\rangle - R)\Big] \approx exp\Big[-k_o^2 4C_\theta{}^2\langle\zeta_o^2\rangle\Big(\frac{\Delta x^2+\Delta y^2}{l^2}\Big)\Big] \tag{4.5}$$

where $R \simeq \langle\zeta_o^2\rangle - \langle\zeta_o^2\rangle\Big(\frac{\Delta x^2+\Delta y^2}{l^2}\Big)$.

Using this approximation, (4.3) can be integrated. The details of the integrations are quite cumbersome and only the result will be shown. The details of this expression need not be looked at too closely, we will only state a few observations for this result. It was used primarily to verify the integration results in the proper regime.

We will define the following in order to simplify the presentation of the result:

$$\alpha_x = \frac{|D_x|^2}{2Re[D_x]} \qquad a_2 = \sqrt{\alpha_x + 2k_o^2C_\theta^2\sigma_y^2 + 2/l^2}$$

$$\alpha_y = \frac{|D_y|^2}{2Re[D_y]} \qquad b_2 = \alpha_y + 2k_o^2C_\theta^2\sigma_y^2 + 2/l^2$$

$$a_1 = \alpha_x + 2k_o^2C_\theta^2\sigma_y^2 + 1/l^2 \qquad a_3 = \alpha_x + 2k_o^2C_\theta^2\sigma_y^2$$

$$b_1 = \alpha_y + 2k_o^2C_\theta^2\sigma_y^2 + 1/l^2 \qquad b_3 = \alpha_y + 2k_o^2C_\theta^2\sigma_y^2. \tag{4.6}$$

Here, σ_y^2 is the variance of slopes and l is the correlation length.

After performing the integration in (4.3), we obtain

$$\langle\vec{E}_s\cdot\vec{E}_s{}^*\rangle = Q\,\frac{\pi}{2Re[D_x]\,C_\theta}$$

$$\left(\frac{\pi}{\sqrt{a_1b_1}}\,exp\left[\frac{-k_o^2S_\theta^2}{b_1}\right]\left\{\frac{8k_o^2S_\theta^2\sigma_y^2}{2b_1}\left(\frac{(S_\theta^2/l^2)}{b_1}+C_\theta^2\right)-\frac{(\sigma_y^2S_\theta^2/l^2)}{b_1}+S_\theta^2\sigma_y^2\right\}\right.$$

$$\left.+\frac{\pi}{\sqrt{a_2b_2}}\,exp\left[\frac{-k_o^2S_\theta^2}{b_2}\right]\left\{\frac{4k_o^2C_\theta^2S_\theta^2\sigma_y^4}{2b_2}\left(\frac{4k_o^2S_\theta^2}{2b_2}-1\right)\right\}+\frac{\pi C_\theta^2}{\sqrt{a_3b_3}}\,exp\left[\frac{-k_o^2S_\theta^2}{b_3}\right]\right). \tag{4.7}$$

Some observations about this result will be mentioned. We note that for a Gaussian correlation function, the variance of the slopes σ_y^2 equals to $\frac{2\langle\zeta_o^2\rangle}{l^2}$ when the expected value of the slopes is zero. All the terms of the asymptotic solution of (4.3) are multiplied by the variance of the heights (through σ_y^2) except one. In fact looking at (4.4) we note that R_{yy} and R_y both are multiplied by the variances of the height. The one term not multiplied by the height variance is the ${C_\theta}^2$ term, which is the coherent component of the mean squared field. Seeing this term is a good check, for when $l^2 \to \infty$, the undulating plane result is what is left.

In the calculation of the NRCS, many authors subtract the mean field squared from the mean squared field before integrating the Δx and Δy coordinates' infinite plane. For plane waves, this is essential in order for the integration to yield a meaningful result. The beam solutions have the advantage of having finite energy and $\langle \vec{E}_s \cdot \vec{E}_s{}^* \rangle$ can be integrated independently.

4.4 Fourth Moment of Scattered Field

The next quantity which is of interest is the fourth moment of the scattered field. The fourth moment is defined as

$$M_4 = \langle (\vec{E}_s \cdot \vec{E}_s{}^*)(\vec{E}_s \cdot \vec{E}_s{}^*) \rangle.$$

This expression can be generated by using equation (4.2) for each of the dot products with the result that

$$M_4 = c\Bigg\langle \int_{-\infty}^{\infty} \cdots \int_{-\infty}^{\infty} \left\{S_\theta{}^2\, \zeta_{yo}\zeta_{y1} + C_\theta S_\theta(\zeta_{yo} + \zeta_{y1}) + C_\theta{}^2\right\}\left\{S_\theta{}^2\, \zeta_{y2}\zeta_{y3} + C_\theta S_\theta(\zeta_{y2} + \zeta_{y3}) + C_\theta{}^2\right\}$$

$$exp\Big[jk_o 2C_\theta(\zeta_o - \zeta_1) - jk_o 2S_\theta(y_o - y_1)\Big] exp\Big[jk_o 2C_\theta(\zeta_2 - \zeta_3) - jk_o 2S_\theta(y_2 - y_3)\Big]$$

$$exp\Big[-(D_x x_o^2 + D_y y_o^2) - (D_x{}^* x_1^2 + D_y{}^* y_1^2)\Big] exp\Big[-(D_x x_2^2 + D_y y_2^2) - (D_x{}^* x_3^2 + D_y{}^* y_3^2)\Big]$$

$$dx_o dy_o dx_1 dy_1 dx_2 dy_2 dx_3 dy_3 \Bigg\rangle,$$

where $c = \left[\left(\frac{k_o \eta\, |H_{o_t}|}{2\pi r_r}\right)^2 (A^2 + B^2)\right]^2$.

The averaging required for the expected values of the equation above are quite extensive and beyond the scope of this thesis. However, this equation can form the starting point for further studies of the effects of beam illumination on the fourth moment.

CHAPTER 5

EVALUATION OF THE GAUSSIAN BEAM NRCS

As shown in section (3.1), the NRCS is formed by using both $\langle \vec{E}_s \rangle$ and $\langle \vec{E}_s \cdot \vec{E}_s^* \rangle$ in

$$\sigma^o = \lim_{r_r \to \infty} \frac{4\pi {r_r}^2 \left(\langle \vec{E}_s \cdot \vec{E}^*{}_s \rangle - \langle \vec{E}_s \rangle \cdot \langle \vec{E}_s^* \rangle \right)}{\int_{-\infty}^{\infty} \int_{-\infty}^{\infty} | E_i |^2 ds_o}.$$

The coherent part of the NRCS, namely $\langle \vec{E}_s \rangle \cdot \langle \vec{E}_s^* \rangle$, was derived in equation (3.7) and requires no further integration, only evaluation for different surface statistics, incident angles and source sizes. The equation for the total backscattered power under a Gaussian beam illumination has been derived in equation (4.4); it requires the numerical evaluation of a two dimensional integral. We must also find the normalization factor $\int_{-\infty}^{\infty} \int_{-\infty}^{\infty} | \vec{E}_i |^2 ds_o$. This normalization factor is found by integrating the incident power over the mean surface. This value for our Gaussian beam illumination is found to be $\frac{\pi W^2 (A^2 + B^2)}{2C_\theta}$.

Normalizing equation (4.4) with,

$$W = n\lambda \qquad l^2 = s^2\lambda^2 \qquad r_r = u\lambda$$
$$\Delta x = p\lambda \qquad \langle \zeta_o^2 \rangle = t^2\lambda^2 \qquad z_d = v\lambda$$
$$\Delta y = q\lambda$$

and simplifying we obtain

$$\sigma^o = \left\{ (4\pi) \int_{-\infty}^{\infty} \int_{-\infty}^{\infty} \left\{ \left[-\left\{ \frac{-2t^2}{s^2} \left(1 - \frac{2q^2}{s^2} \right) exp\left[\frac{-(p^2+q^2)}{s^2} \right] \right.\right.\right.$$

$$\left. + \left(\frac{64\pi^2 C_\theta^2 \, t^4 q^2}{s^4} \right) exp\left[\frac{-2\,(p^2+q^2)}{s^2} \right] \right\} S_\theta^2 + C_\theta^2 \Bigg] cos(4\pi S_\theta q)$$

$$\left. - \left(\frac{-16\pi C^2{}_\theta S_\theta t^2 q}{s^2} \right) exp\left[\frac{-(p^2+q^2)}{s^2} \right] sin(4\pi S_\theta q) \right\}$$

$$exp\left[-D_{cxn}(p^2+q^2) \right] exp\left[-D_{cyn}(p^2+q^2) \right]$$

$$exp\left[-16\pi^2 C_\theta t^2 \left(1 - exp\left[\frac{-(p^2+q^2)}{s^2} \right] \right) \right] dpdq$$

$$\left. - 8\pi^2 C_\theta n^2 exp\left[-16\pi^2 C_\theta t^2 \right] exp\left[-\pi^2 S_\theta^2 C_\theta^2 n^2 \right] \right\} \tag{5.1}$$

where

$$D_{cxn} = \left(\frac{|\, D_x \,|^2}{2\mathrm{Re}[D_x]} \right) = \frac{\left(\dfrac{(2\pi n)^2}{(2\pi)^2 n^4 + 4v^2} \right)^2 + \left(\dfrac{4\pi v}{(2\pi)^2 n^4 + 4v^2} + \dfrac{\pi}{u} \right)^2}{\dfrac{2(2\pi n)^2}{(2\pi)^2 n^4 + 4v^2}}$$

and

$$D_{cyn} = \left(\frac{|\, D_y \,|^2}{2\mathrm{Re}[D_y]} \right) = \frac{\left(\dfrac{C_\theta^2 \, (2\pi n)^2}{(2\pi)^2 n^4 + 4v^2} \right)^2 + \left(\dfrac{C_\theta^2 \, 4\pi v}{(2\pi)^2 n^4 + 4v^2} + \dfrac{\pi}{u} \right)^2}{\dfrac{2C_\theta^2 \, (2\pi n)^2}{(2\pi)^2 n^4 + 4v^2}}.$$

Numerical evaluation of the above integrals can be performed using two single integration routines in tandem. One routine is especially suited to highly

oscillatory integrals (which are present due to the $cos(4\pi S_\theta q)$ and the $sin(4\pi S_\theta q)$ terms), while the other integration routine is simply a Gauss-Kronrod quadrature routine for adaptive integration. Adaptive integration routines will successively break down an integration into smaller and smaller steps until given tolerances of accuracy are reached. The computer code used was a modification of the Quadpack integration routines. The source code was changed in order to allow for the integration routines to call functions which contained another integration call. The code was tested and verified for several analytically solvable two-dimensional integrals.

The validity of the answers that we obtain are governed by how well we keep within the approximations made to derive the σ^o expression. The accuracy of the approximations to the plane wave spectrum approach that gave the field radiated by the illuminating source have been explored by many authors [2,16,17,18]. Using criteria given by Agrawal and Pattanayak[17], a minimum waist size for which the Gaussian beam will be a valid radiation solution is conservatively $W \approx 10\lambda$. This will be a constraint on how small the source can be.

The Kirchhoff approximation, used for the determination of the surface current density, has its own inherent limitations. From Ogilvy[3], the following ratios must be large for the approximation to be valid; l/λ and $l/\sqrt{\langle c_o^2 \rangle}$. Also, the angle of the incident field must be within 10° off normal; this further strengthens the accuracy of Kirchhoff approximation. Additional simplifications are introduced due to the approximation of the Green's Function. Since the observation point is tending to infinity, the Green's Function approximation will be valid. There is, however, a limitation on the maximum dimension of the source size. It is known that the source field will diffract on its propagation

down to the rough surface. The field, or current induced on the surface, can be considered as another source. Therefore, we must realize that the source waist size cannot become infinite for this would even violate the regime in which the Fresnel approximation to the Green's Function is valid. In summary, the constraints on the parameters in our solution are

Constraint	Reason
$W > 10\lambda$	-validity of radiation form source.
$l/\lambda \gg 1,\ l/\sqrt{\langle \zeta_o^2 \rangle} \gg 1,\ 0^\circ \leq \theta_i \leq 10^\circ$	-validity of Kirchhoff approximation.
$k_o r_r \gg 1$ and $W \ll \infty$	- validity of the Green's function approximation.

Using these guidelines, we ran several cases computing the NRCS versus varying beam size and surface statistics. The results of this study will be shown and discussed in the Results and Conclusions section of this thesis.

Chapter 6

EVALUATION OF GAUSSIAN TAPERED WAVE NRCS

As stated in the abstract, we note that the derivation for the Gaussian beam can be used for an assumed incident field on the surface comprising a plane wave with a Gaussian amplitude taper. The form of this field will not be derived from a source as was the Gaussian beam solution; however, this field could possibly be formed by using a lens or inverse phasing. The field incident on the random PEC, with the coordinate transformations already taken into account, is given as

$$\vec{H}_i = \frac{\left\{B\hat{x}_o + A(C_\theta \hat{y}_o + S_\theta \hat{z}_o)\right\}}{\eta} exp\Big[- jk_o(y_o S_\theta - \zeta_o C_\theta) - D\Big(x_o^2 + (y_o C_\theta + \zeta_o S_\theta)^2\Big)\Big].$$

Again, as in the case of the Gaussian beam solution, we neglect the quadratic random height dependence. This expression used in the Kirchhoff approximation and for backscatter reduces to the following expression for the $\langle \vec{E}_s \rangle$

$$\langle \vec{E}_s \rangle = \frac{-jk_o}{2\pi r_r} exp[-jk_o r_r]\, exp\Big[-2k_o^2 C_\theta^2 \langle \zeta_o^2 \rangle\Big] exp\left[-\frac{k_o^2}{D} S_\theta^2\right]$$

$$\frac{\pi}{DC_\theta}\left\{-\hat{x}_o AC_\theta + \hat{y}_o BC_\theta^2 + \hat{z}_o BS_\theta C_\theta\right\}.$$

The averaging was performed in the same manner as in the Gaussian beam case. This expression is very similar to equation (3.6), except that the amplitude multiplier has no source distance information and D is a real quantity. The formation of $\langle \vec{E}_s \rangle \cdot \langle \vec{E}_s^* \rangle$ is needed for the NRCS and is found to be

$$\langle \vec{E}_s \rangle \cdot \langle \vec{E}_s^* \rangle = \frac{k_o^2 (A^2 + B^2)}{4r_r^2 D} exp\Big[-4k_o^2 C_\theta^2 \langle \zeta_o^2 \rangle\Big] exp\left[-\frac{2k_o^2}{D} S_\theta^2\right]. \qquad (6.1)$$

Next we consider the total power calculation, $\langle \vec{E}_s \cdot \vec{E}_s^* \rangle$. Once again, the similarities are straightforward and the final result can simply be found by inspection of the Gaussian beam result equation in (4.4), noting the modifications in the constant multiplier, and that D is real, i.e.

$$\langle \vec{E}_s \cdot \vec{E}_s^* \rangle = \frac{k_o^2 (A^2 + B^2)}{\pi 8 r_r^2 D C_\theta} \int_{-\infty}^{\infty} \int_{-\infty}^{\infty} \Big\{ \Big[-(R_{yy} + R_y{}^2 k_o^2 4 C_\theta{}^2) S_\theta{}^2 + C_\theta{}^2 \Big] cos(k_o 2 S_\theta \Delta y)$$

$$- 4 R_y k_o C_\theta{}^2 S_\theta sin(k_o 2 S_\theta \Delta y) \Big\}$$

$$exp\Big[-\frac{D}{2} \Delta x^2 \Big] exp\Big[-\frac{DC_\theta^2}{2} \Delta y^2 \Big]$$

$$exp\Big[-k_o^2 4 C_\theta{}^2 (\langle \zeta_o^2 \rangle - R) \Big] d\Delta x d\Delta y. \qquad (6.2)$$

Next we must find the normalization factor for the RCS, namely $\int_{-\infty}^{\infty} \int_{-\infty}^{\infty} |\vec{E}_i|^2 ds_o$. The expression for the $|\vec{E}_i|^2$ can be found to be

$$|\vec{E}_i|^2 = (A^2 + B^2) exp\Big[-2D\Big(x_o^2 + y_o^2 C_\theta^2 \Big) \Big].$$

Therefore, by some simple integration the normalization factor is $(A^2 + B^2)\frac{\pi}{2DC_\theta}$. We now have all the components to form the NRCS expression. The integral of equation (6.2) can be normalized, as was done for the Gaussian beam, by the wavelength. The following substitutions will be recalled, where we now have D as our attenuation factor:

$$D = m\lambda^2 \qquad l^2 = s^2\lambda^2 \qquad r_r = u\lambda$$
$$\Delta x = p\lambda \qquad \Delta y = q\lambda \qquad \langle \zeta_o^2 \rangle = t^2\lambda^2.$$

Using these and the other expressions derived above yields

$$\sigma^o = \left\{(4\pi)\int_{-\infty}^{\infty}\int_{-\infty}^{\infty}\left\{\left[-\left\{\frac{-2t^2}{s^2}\left(1-\frac{2q^2}{s^2}\right)exp\left[\frac{-(p^2+q^2)}{s^2}\right]\right.\right.\right.$$

$$\left.\left.+\left(\frac{64\pi^2 C_\theta^2\, t^4 q^2}{s^4}\right)exp\left[\frac{-2\,(p^2+q^2)}{s^2}\right]\right\}S_\theta^2 + C_\theta^2\right]cos(4\pi S_\theta q)$$

$$\left.-\left(\frac{-16\pi C^2{}_\theta S_\theta t^2 q}{s^2}\right)exp\left[\frac{-(p^2+q^2)}{s^2}\right]sin(4\pi S_\theta q)\right\}$$

$$exp\left[-m(p^2+q^2)\right]exp\left[-mC_\theta^2(p^2+q^2)\right] \qquad (6.3)$$

$$exp\left[-16\pi^2 C_\theta t^2\left(1-exp\left[\frac{-(p^2+q^2)}{s^2}\right]\right)\right]dpdq$$

$$\left.-\frac{8\pi^2 C_\theta}{m^2}exp\left[-16\pi^2 C_\theta t^2\right]exp\left[-\frac{\pi^2 S_\theta^2 C_\theta^2}{m^2}\right]\right\}.$$

Evaluation of this expression, once again, requires the use of a two-dimensional integration routine. The program for calculating the above NRCS was generated by changing the appropriate equations for the Gaussian beam result. The only constraints on the analysis now arise from our use of the Kirchhoff approximation for the surface current and the approximation in the calculation of the field radiated by these currents. The bounds are given at the end of Chapter 5. In the results and conclusions section we shall discuss the NRCS as we vary the correlation length and spot size of the illuminated area on the surface.

Chapter 7

RESULTS AND CONCLUSIONS

7.1 Gaussian Beam Illumination

The derivation of the NRCS with a Gaussian beam illumination using the Kirchhoff approximation was given in Chapters 2-5. In this section we will present the results of the numerical evaluation of the NRCS and show how it compares to plane wave illumination [3] whose derivation is presented in Appendix E. The plane wave result derived in Appendix E circumvents the averaging of the slope terms we performed using the Stochastic Fourier Transform by resorting to an integration by parts to eliminate the slopes [3,13]. The limitation in performing integration by parts is that in order to complete the derivation we must assume the surface has an illumination that is many correlation lengths in extent. The averages we perform in this thesis have no such restriction.

The motivation behind using the beam solution as an incident field is to try to understand the effect of spot size in rough surface scattering. As stated previously, equation (4.4) allows us to see the dependence on the surface height autocorrelation function not only in the exponential, but also in the other amplitude terms. Integration by parts under the many correlation lengths illumination assumption only contains the autocorrelation function in the exponential term. It was found that each of the terms in equation (4.4) is significant, and in order for the plane wave NRCS to match the Gaussian beam solution, they must all be included.

To present the NRCS calculations, we plot this quantity versus beam radius at the surface normalized to a correlation length. The beam radius is defined as the radius at which the incident field amplitude has fallen to the e^{-1} point. This will show how the NRCS is affected by changing the illumination spot size.

A plot of the backscattered NRCS versus incident beam radius is shown in figure 7.1a. We see a sharp rise in the NRCS as the beam radius increases. This is attributed to the phase of the Gaussian beam on the surface. The beam radius on the surface is defined as $\frac{1}{\sqrt{\mathrm{Re}[D]}}$, and is normalized by the correlation length, where D is the beam radius at the surface see figure 7.0 (D is defined in the statement of our incident field). Careful inspection of the functional dependence of D on the source beam radius, W, shows that D can have the same value for two different values of W. Thus, the multivaluedness of D, upon varying our source size, causes the NRCS to become multivalued as well. We note that while two different values of W will give the same amplitude taper on the surface, the phase fronts will be different (see figure 7.0). We note that the quadratic phase on the surface for large W is more planar than for a smaller W (a more indepth discussion of this is contained in Appendix G). A graph of the NRCS where we have neglected the quadratic phase of the Gaussian beam is also shown in figure 7.1a along with the plane wave NRCS. As the beam waist on the surface becomes large compared to a correlation length the surface is being "fully illuminated," that is, it is being illuminated sufficiently such that the statistics of the illuminated surface adequately represent the entire surface realization. This is the regime where the plane wave and Gaussian beam illumination match.

Plots of the NRCS are presented in figures 7.1a-d, for various incident angles, surface heights, and correlation lengths. All the plots show the initial phase effect and all approach the plane wave result as the beam radius becomes large. Note in the first two figures, 7.1a-b, that in varying the incident angle, keeping the surface statistics fixed, the backscattered field falls dramatically as we move from normal. This is expected given the small variance of the slopes. A surprising result is shown in figures 7.1c and 7.1d. As the correlation length increases from 7.1c to 7.1d, where we have fixed the surface height variance and

incident angle, we see that the NRCS actually increases. One might expect that the longer correlation length would yield a smaller NRCS because the surface is becoming smoother. The affect of the longer correlation length is that incoherent power diminishes at angles further off the normal and is redistributed into a more normal direction. The well known fact that the NRCS is highly slope dependent is further corroborated by this effect.

In conclusion, a model for Gaussian beam random rough surface scattering under the Kirchhoff approximation for a Gaussian height and slopes distributed surface has been presented. A significant transition region for the NRCS when the surface is illuminated by a Gaussian beam, due to phase and taper affects of the beam, have been found. The model may be used in the future as a check of Monte Carlo 3-D simulations when they become available. However current computer requirements for the 3-D problem are too intensive. The solution may also be used in the optics regime, since the aperture distribution assumed has been used as a crude approximation to the aperture distribution of a laser.

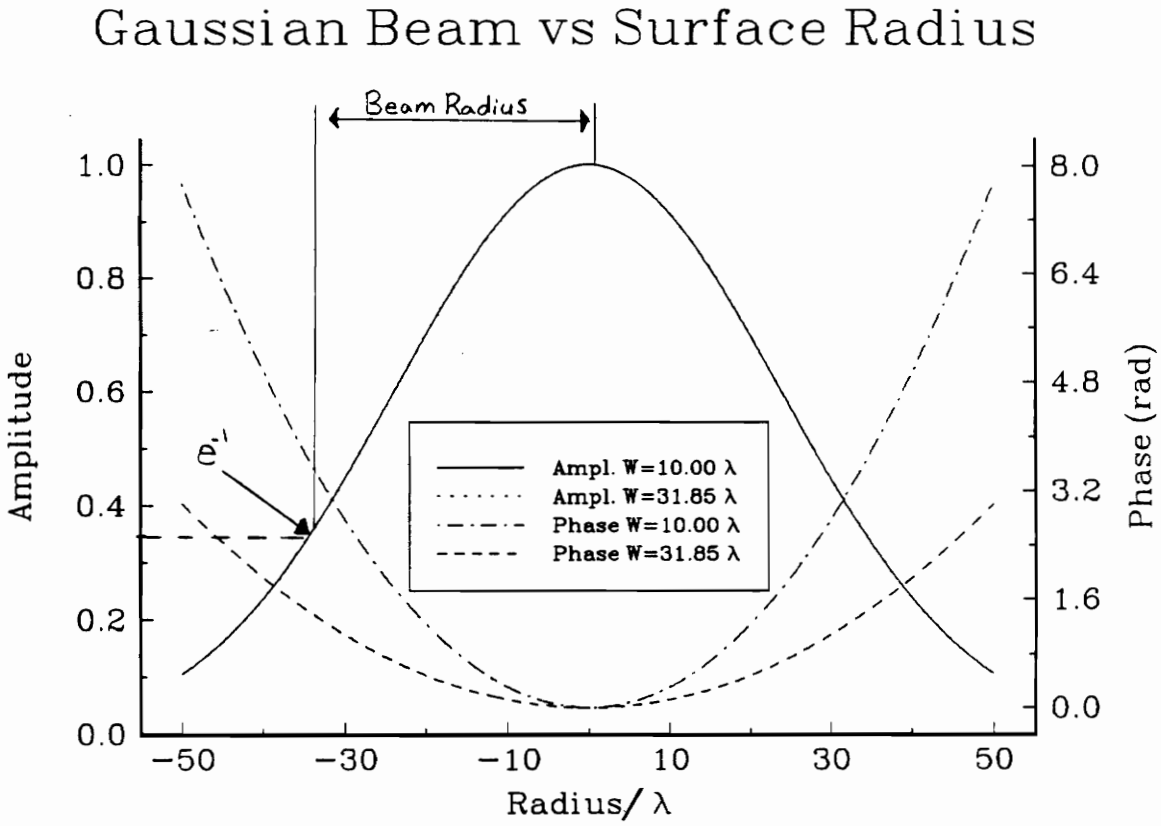

Figure 7.0 Gaussian Beam Spot Size and Phase- The following parameters were used: $\theta_i = 0$ deg, $z_d = 1000$, $W = 10.00\lambda$ and $W = 31.85\lambda$.

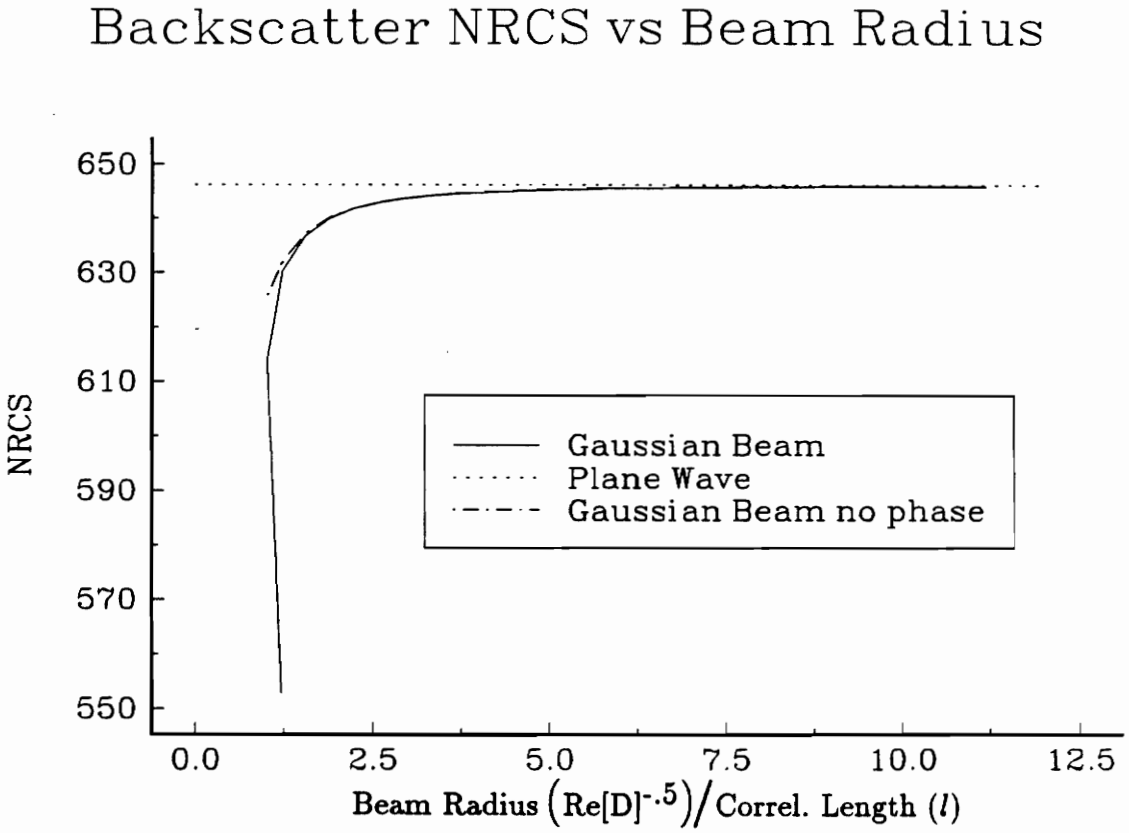

Figure 7.1a Backscatter NRCS vs Beam Radius- The following parameters were used: $\theta_i = 0$ deg, $z_d = 800\ \lambda$, $r_r = 2 \times 10^{15}\ \lambda$, $\langle \zeta^2 \rangle = .2\ \lambda^2$ and $l^2 = 500\ \lambda^2$.

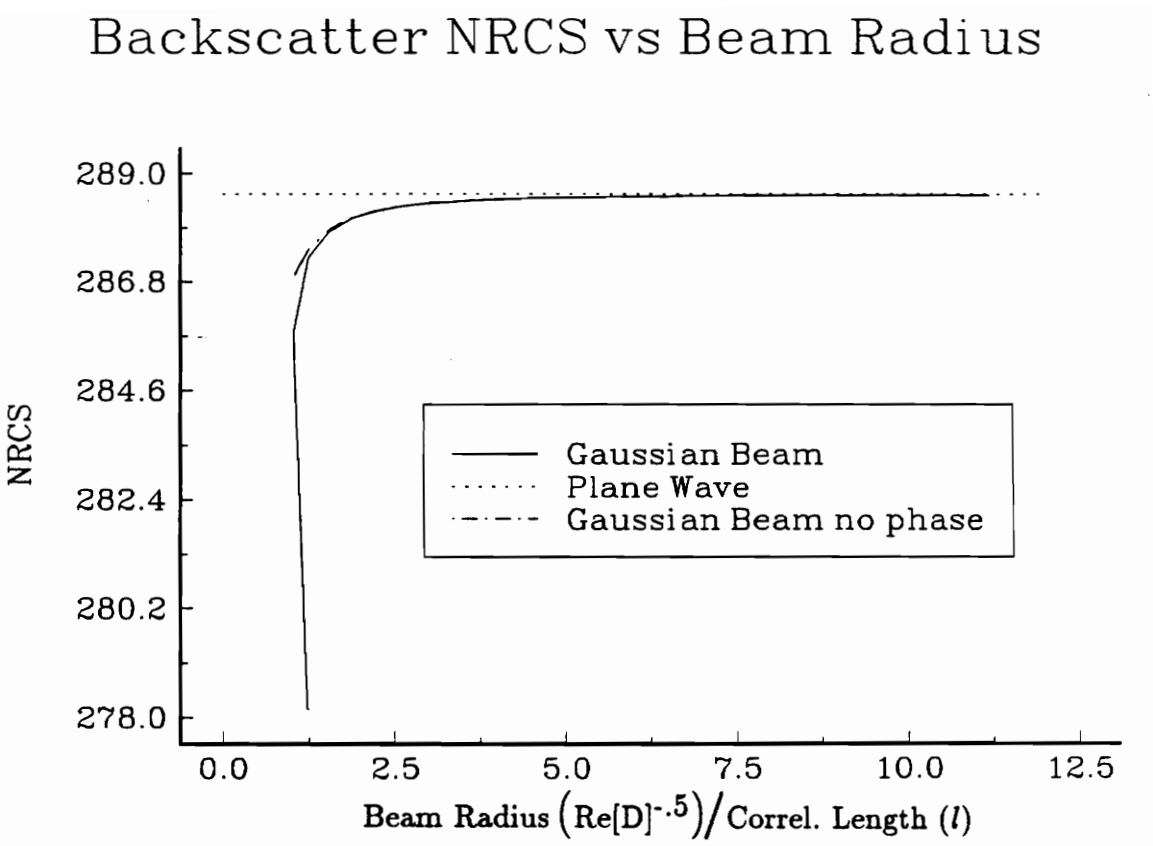

Figure 7.1b Backscatter NRCS vs Beam Radius- The following parameters were used: $\theta_i = 2.0$ deg, $z_d = 800\ \lambda$, $r_r = 2 \times 10^{15}\ \lambda$, $\langle \zeta^2 \rangle = .2\ \lambda^2$ and $l^2 = 500\ \lambda^2$.

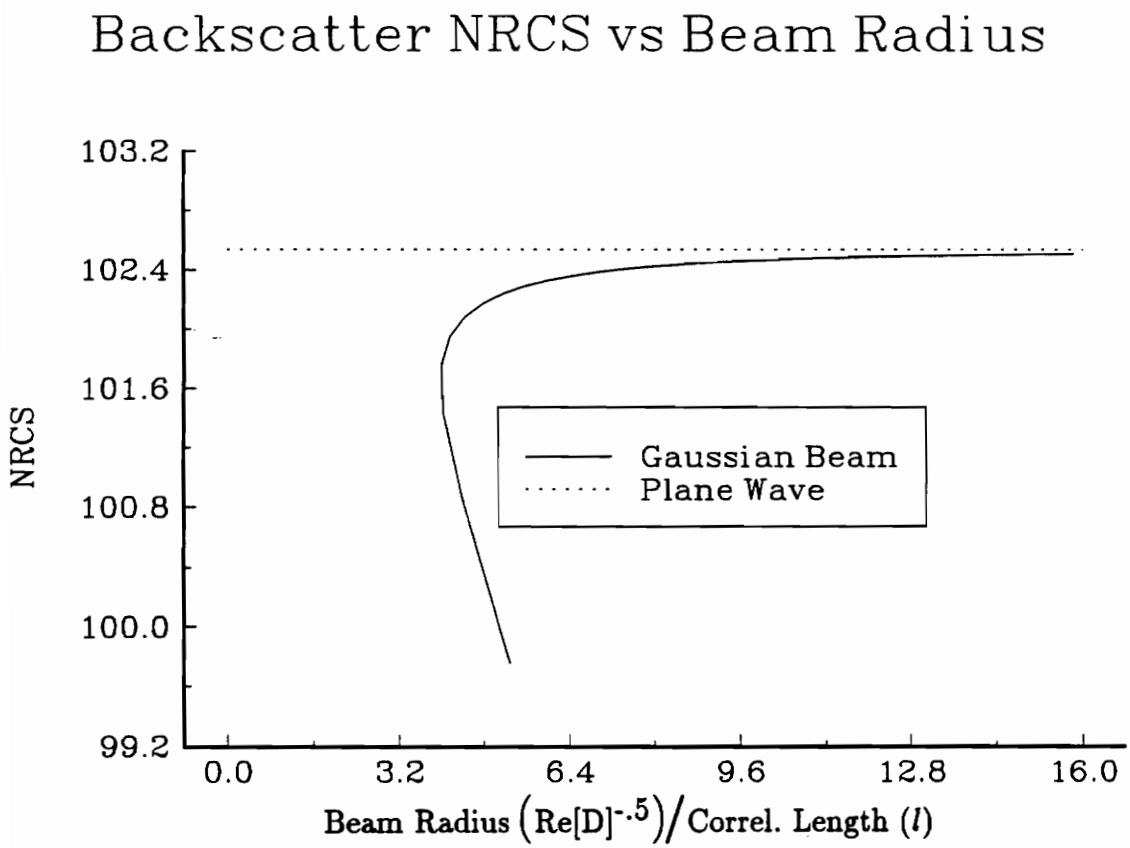

Figure 7.1c Backscatter NRCS vs Beam Radius- The following parameters were used: $\theta_i = 1.15$ deg, $z_d = 1000\ \lambda$, $r_r = 2 \times 10^8\ \lambda$, $\langle \zeta^2 \rangle = .1\ \lambda^2$ and $l^2 = 40\ \lambda^2$.

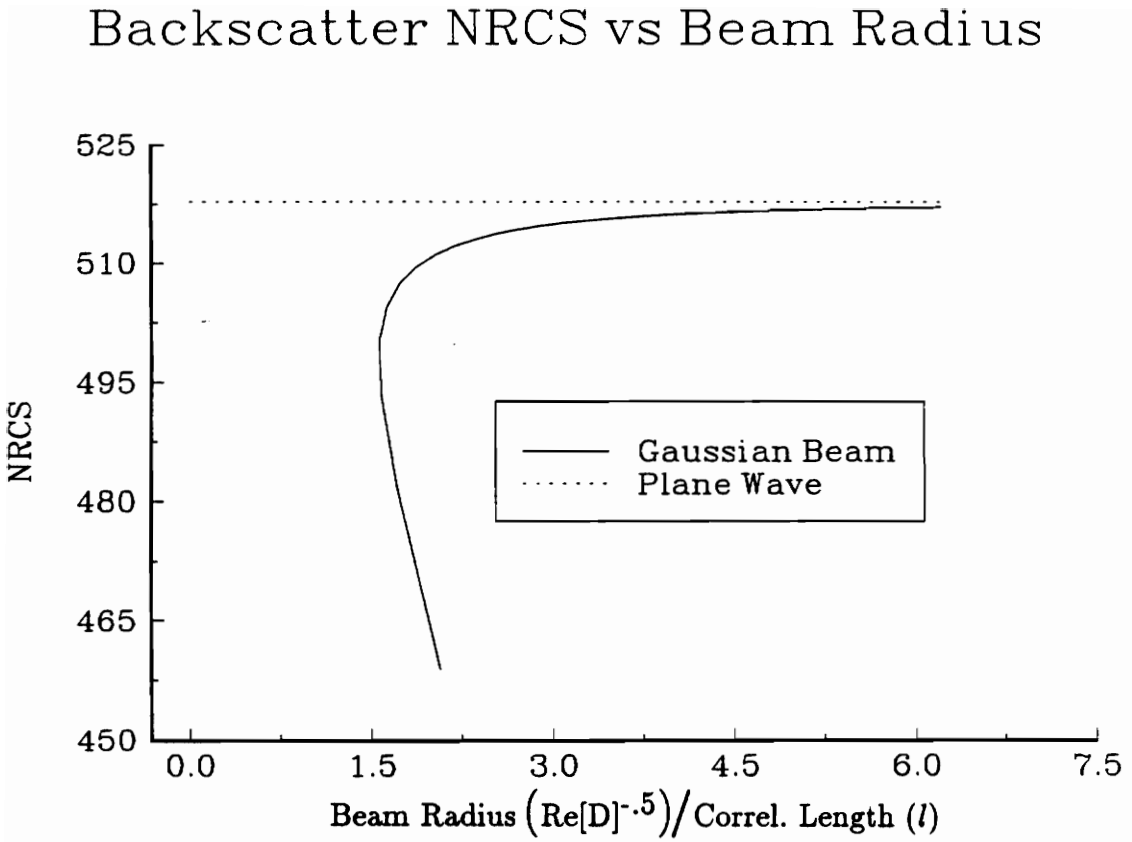

Figure 7.1d Backscatter NRCS vs Beam Radius- The following parameters were used: $\theta_i = 1.15$ deg, $z_d = 1000\ \lambda$, $r_r = 2 \times 10^8\ \lambda$, $\langle \zeta^2 \rangle = .1\ \lambda^2$ and $l^2 = 260\ \lambda^2$.

7.2 Gaussian Tapered Plane Wave Illumination

The results for a Gaussian tapered plane wave can provide additional insight into the effect of under illumination of the surface by the incident field. By eliminating the phase effect which is inherent in the Gaussian beam solution, we can isolate how a simple amplitude taper affects the NRCS. The parameter D in our assumed surface amplitude taper, $exp\left[-D(x^2+y^2)\right]$, will be varied to show how the NRCS reacts when only the amplitude of the field illumination is considered. The complex integral expression shown in equation (6.3) will be used to indicate how much of the surface must be illuminated in order to obtain an accurate representation of the surface statistics.

Since our incident field has a taper of the form $exp\left[-D(x^2+y^2)\right]$, we will define the incident field beam radius to be the value $\frac{1}{\sqrt{\mathrm{Re}[D]}}$ and normalize it to a correlation length, as was done for the Gaussian beam case. We show plots of the backscatter NRCS vs. the incident field beam radius in units of correlation length (Figures 7.2a-c).

These graphs show that the Gaussian tapered plane wave NRCS does not produce the plane wave NRCS until the beam radius is approximately 10 correlation lengths. These results could be used to determine a surface's correlation length by varying the illumination spot size. Specifically, by varying the spot size on the surface we could generate a plot of the NRCS vs Beam Radius and obtain an estimate of the correlation length from the transition region which is seen in the theoretical results. The Gaussian beam results show the same trend.

Finally, the Gaussian tapered plane wave results provide a simple way of determining the effect of beam width on the scattered field. However, as stated earlier, the synthesis of such an incident field will be difficult to accomplish. The results shown here have demonstrated that one may model the random

rough surface scattering and under certain conditions derive surface characteristics by varying the illumination spot size. A possible technique for utilizing the model is as follows. The coherent power, being dominated by the rms surface height, could be measured in the plane wave limit and compared against theoretically derived results. Once the rms height is known, the NRCS model could be run for various correlation lengths and compared with the measurement of the scattered field (or NRCS), where the surface is illuminated with a small spot size and the spot size is increased until a constant value of the NRCS is measured. The major limitations of this method are that the surface would have to be a PEC and have the assumed statistics of this model. If the Gaussian surface statistics can be reasonably assumed for a surface one could incorporate a lumped loss due to the reflection coefficients introduced by a non PEC and thereby use this model to determine surface rms height and slope.

The phenomenon of the NRCS dropping under illumination thus far has simply been observed and not explained. The reason why this drop occurs is that the illuminated surface no longer represents the overall surface. The statistics for a small spot size no longer match the overall surface. Investigation of the statistics of the sample of surface being illuminated can be done by numerically generating a realization of a surface, with the assumed surface correlation length and rms height, and then window a portion of the data generated and compute the statistics of this windowed portion. A preliminary study using this approach was performed. The autocorrelation function of the windowed portion no longer was Gaussian and the correlation length was considerably shorter. The shorter correlation length does support the decreasing value of the NRCS value. Our term "under illumination" can now be further defined. We consider this to be the point where the taper has altered the statistics by having windowed in on too small a portion of the surface.

To conclude, we have furthered the study of random rough surfaces by deriving a more realistic and more probing model of surface scattering in the Kirchhoff limit. The use of the Stochastic Fourier Transform allows us to overcome the classical constraint that a surface must be illuminated by many wavelengths in order to complete the scattering calculation. The use of a Gaussian beam source allows for a more physically obtainable illumination of the source. These qualities have not been studied in this limit to this author's knowledge.

The advances in computing power have helped make the final evaluation of the model feasible. All calculations for both Gaussian beam illumination and Gaussian tapered plane wave, were run on an IBM compatible 486 33 MHz PC with a Weitek math coprocessor. Also, as a check, the programs were run on an IBM compatible 486 50 MHz PC with an i860 vector processor board. Execution of the code was approximately 1.5 time faster on the i860 board even without vectorization. The Quadpack quadratures are not amenable to vectorization due to the modularized code and decision statements involved in the calculations.

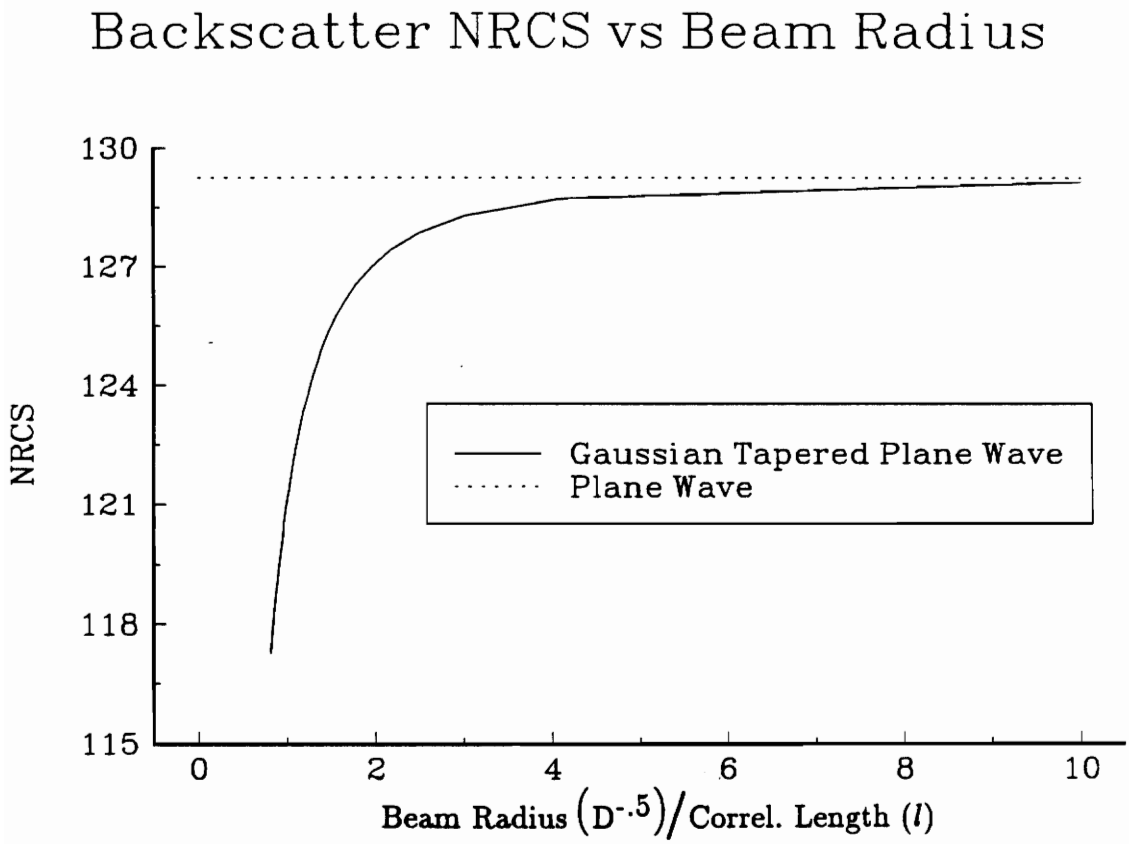

Figure 7.2a Backscatter NRCS vs Beam Radius- The following parameters were used: $\theta_i = 0$ deg, $z_d = 800\ \lambda$, $r_r = 2 \times 10^{15}\ \lambda$, $\langle \zeta^2 \rangle = .2\ \lambda^2$ and $l^2 = 100\ \lambda^2$.

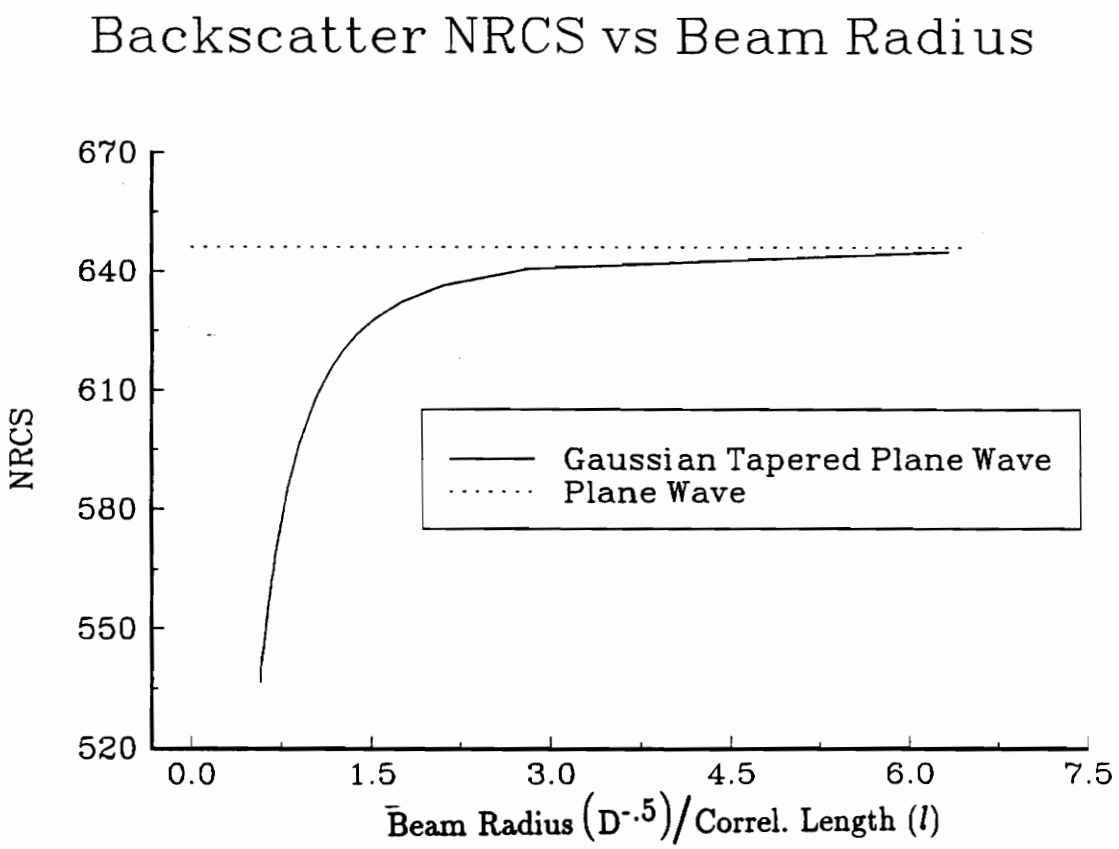

Figure 7.2b Backscatter NRCS vs Beam Radius- The following parameters were used: $\theta_i = 0$ deg, $z_d = 800\ \lambda$, $r_r = 2 \times 10^{15}\ \lambda$, $\langle \zeta^2 \rangle = .2\ \lambda^2$ and $l^2 = 500\ \lambda^2$.

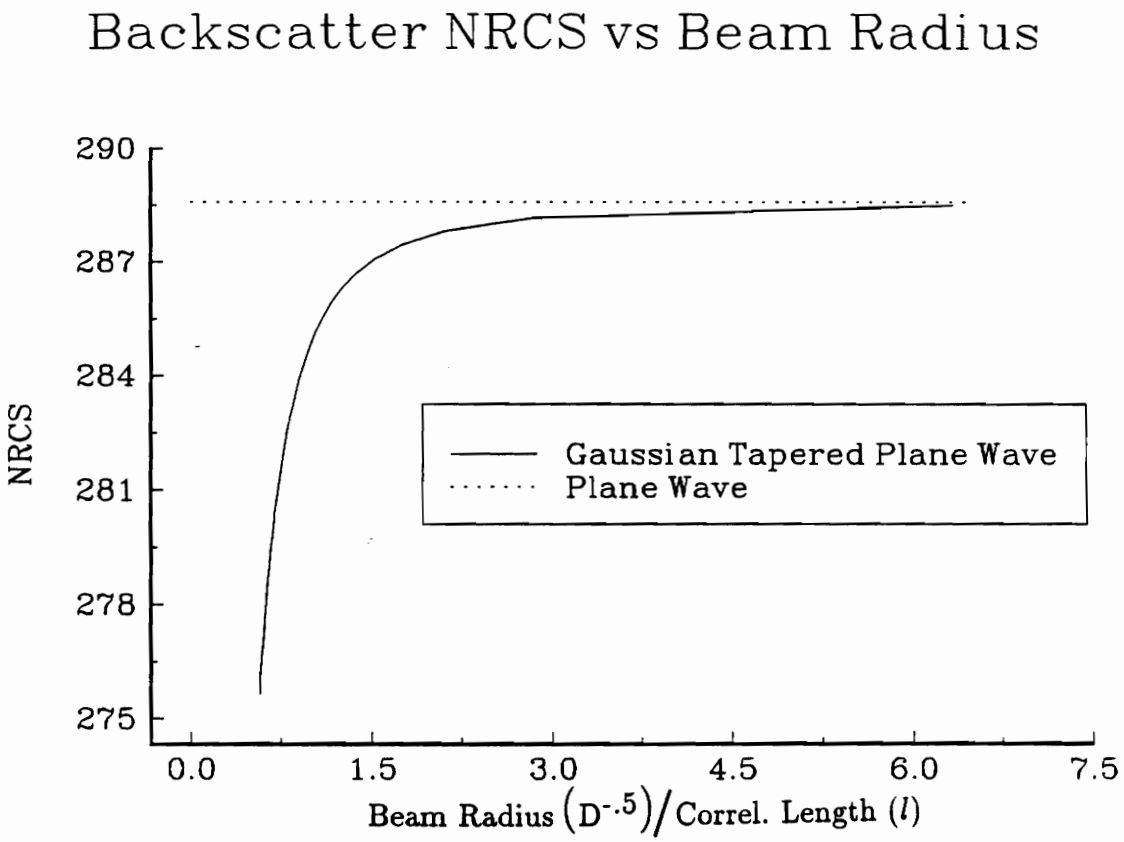

Figure 7.2c Backscatter NRCS vs Beam Radius- The following parameters were used: $\theta_i = 2.0$ deg, $z_d = 800\ \lambda$, $r_r = 2 \times 10^{15}\ \lambda$, $\langle \zeta^2 \rangle = .2\ \lambda^2$ and $l^2 = 500\ \lambda^2$.

REFERENCES

[1] R. E. Collin, Antennas and Radiowave Propagation, New York: McGraw-Hill, 1985.

[2] J. Tuovinen, "Accuracy of a Gaussian Beam," IEEE Trans. Antennas Propagat., Vol. 40, No. 4, pp. 391-398, April 1992.

[3] J. A. Ogilvy, Theory of Wave Scattering from Random Rough Surfaces, Adam Hilger, New York, 1991.

[4] R. D. Kodis, "A Note on the Theory of Scattering from an Irregular Surface," IEEE Antennas Propagat., Vol. AP-14, No. 1, pp. 77-82, January 1966.

[5] A. Stogryn, "Electromagnetic Scattering Form Rough, Finitely Conducting Surfaces," Radio Science, Vol. 2, No. 4, pp. 415-428, April 1967.

[6] P. Beckman and A. Spetzichino, The Scattering of Electormagnetic Waves From Rough Surfaces, Pergamon Press, New York, 1963.

[7] G. S. Brown, EE 5105-6 Class Notes.

[8] W. L. Stutzman and G. A. Theile, Antenna Theory and Design, John Wiley & Sons, New York, 1981.

[9] E. I. Thorsos and D. R. Jackson, "Studies of scattering theory using numerical methods," Waves in Random Media, Vol. 3, pp. S165-S190, 1991.

[10] G. S. Brown, "A Comparison of Approximate Theories for Scattering from Rough Surfaces," Wave Motion, Vol. 7, pp. 195-205, 1985.

[11] G. L. Geernaert and W. J. Plant, eds. Surface Waves and Fluxes, Vol. II, Kluwer Academic Pub., Netherlands, 1990.

[12] M. Abromovitz and I. A. Stegun, eds. Hanbook of Mathematical Functions, Dover Pub., New York, 1965.

[13] I. Tolstoy and C. S. Clay, Ocean Acoustics: Theory and Experiment in Underwater Sound, McGraw-Hill, New York, 1966.

[14] G. S. Brown, "Simplifications in the Stochastic Fourier Transform Approach to Random Surface Scattering," IEEE Trans. Antennas Propagat., Vol. AP-33, No. 1, pp. 48-55, January 1985.

[15] K. S. Shamugan and A. M. Breipohl, Random Signals: Detection, Estimation and Data Analysis, John Wiley & Sons, New York, 1988.

[16] S. Nemoto, "Nonparaxial Gaussian beams," Appl. Opt., Vol. 29, No. 13, pp. 1940-1946, May 1990.

[17] G. P. Agrawal and D. N. Pattanayak, "Gaussian beam propagation beyond the paraxial approximation," J. Opt. Soc. Am., Vol. 69, No. 4, pp. 575-578, April 1979.

[18] A. T. Friberg, T. Jaakkola and J. Tuovinen, "Electromagnetic Gaussian Beam Beyond the Paraxial Regime," IEEE Trans. Antennas Propagat., Vol. 40, No. 8, pp. 984-989, August 1992.

[19] A. Ishimaru, Electromagnetic Wave Propagation, Radiation, and Scattering, Prentice-Hall, New Jersey, 1991.

[20] R. F. Harrington, Time-Harmonic Electromagnetic Fields, McGraw-Hill, New York, 1961.

[21] P. C. Clemmow, Plane Wave Spectrum Representation of Electromagnetic Fields, Pergamon Press, New York, 1966.

[22] L. Felsen and N. Marcuvitz, Radiation and Scattering of Waves, Prentice-Hall, New Jersey, 1973.

[23] J. P. Keener, Principles of Applied Mathematics: Transformations and Approximation, Addison-Wesley, New York, 1988.

[24] G. C. Cooper and C. D. McGillem, Probabilistic Methods of Signal and System Analysis, Holt, Rinehart and Winston, New York, 1986.

[25] H. A. Haus Waves and Fields in Optoelectronics, Prentice-Hall, New Jersey, 1984.

APPENDIX A: PLANE WAVE SPECTRUM APPROACH

Given the tangential fields on a plane, this appendix derives an expression for the electromagnetic fields off this plane. The method we will use is known as the plane wave spectrum approach [1,19,20,21]. We will follow the derivation given by Brown [7].

From Maxwell's equations, we know that in a source free space,

$$\vec{E}(\vec{r}) = \frac{-j\eta}{k_o} \nabla \times (\nabla \times \vec{A}(\vec{r})) \tag{A1}$$

where $k_o = w\sqrt{\mu_o \epsilon}$, $\eta = \sqrt{\frac{\mu_o}{\epsilon_o}}$, $\vec{H} = \nabla \times \vec{A}$ and $\vec{A}$ is the vector magnetic potential. The $exp[j\omega t]$ time dependence is assumed. The magnetic vector potential $\vec{A}(\vec{r})$ is given by

$$\vec{A}(\vec{r}) = \int_{\text{Source}} \vec{J}(\vec{r}_o)\, G(|\vec{r} - \vec{r}_o|)\, dv_o \tag{A2}$$

where $\vec{J}(\vec{r}_o)$ is the source current and $G(|\vec{r} - \vec{r}_o|)$ is the shifted spatial impulse response for $\vec{A}(\vec{r})$ which satisfies,

$$(\nabla^2 + k_o^2)\, G(\vec{r}) = -\delta(\vec{r}).$$

Taking the Fourier transform of this equation results in;

$$((-jk_x)^2 + (-jk_y)^2 + (-jk_z)^2 + k_o^2)\, \tilde{G}(\vec{k}) = -1.$$

The Fourier transform will be defined as:

$$\tilde{f}(k_x) = \int_{-\infty}^{\infty} f(x)\, exp[jk_x x]\, dx = \mathfrak{F}\{f(x)\}$$

and the inverse operation is given as:

$$f(x) = \frac{1}{2\pi} \int_{-\infty}^{\infty} \tilde{f}(k_x)\, exp[-jk_x x]\, dk_x = \mathfrak{F}^{-1}\{f(k_x)\}.$$

Solving for $\tilde{G}(\vec{k})$ results in,

$$\tilde{G}(\vec{k}) = \frac{1}{\vec{k}^2 - k_o^2},$$

where $\vec{k}^2 = k_x^2 + k_y^2 + k_z^2$.

Taking the inverse Fourier transform of $\tilde{G}(\vec{k})$ to recover $G(\vec{r})$ gives,

$$G(\vec{r}) = \frac{1}{(2\pi)^3} \int_{-\infty}^{\infty} \int_{-\infty}^{\infty} exp[-jk_x x - jk_y y] \left\{ \int_{-\infty}^{\infty} \frac{exp[-jk_z z]}{[k_z^2 - (k_o^2 - (k_x^2 + k_y^2))]}\, dk_z \right\} dk_x dk_y.$$

Integration with respect to k_z can be accomplished by letting k_o be slightly complex (lossy medium) in order to move the poles off the real axis; this allows for use of the residue theorem to evaluate the integral. We restrict our solution to be valid for $z \geq 0$. This results in the following form known as the Weyl representation for the free space Green's function:

$$G(\vec{r}) = \frac{1}{(2\pi)^2} \int_{-\infty}^{\infty} \int_{-\infty}^{\infty} \frac{exp\left[-jk_x x - jk_y y - jKz\right]}{j2K} \, dk_x dk_y, \qquad z \geq 0$$

$$\text{where } K = \begin{cases} \sqrt{k_o{}^2 - (k_x{}^2 + k_y{}^2)} \;, & k_o{}^2 > (k_x{}^2 + k_y{}^2) \;. \\ -j\sqrt{(k_x{}^2 + k_y{}^2) - k_o{}^2} \;, & k_o{}^2 < (k_x{}^2 + k_y{}^2) \end{cases}$$

By substituting the Weyl representation of $G(|\vec{r} - \vec{r}_o|)$ in equation (A2), the following form for $\vec{A}(\vec{r})$ results (where $z \geq z_o$ has been assumed);

$$\vec{A}(\vec{r}) = \frac{1}{(2\pi)^2} \int_{-\infty}^{\infty} \int_{-\infty}^{\infty} \left\{ \int_{-\infty}^{\infty} \int_{-\infty}^{\infty} \int_{-\infty}^{\infty} \frac{\vec{J}_s(\vec{r}_o) \exp\left[-j\vec{k}_t \cdot \vec{r}_{t_o} - jKz_o\right]}{j2K} \, dv_o \right\} exp\left[-j\vec{k}_t \cdot \vec{r}_t - jKz\right] d\vec{k}_t$$

Here, $\vec{k}_t = k_x\hat{x} + k_y\hat{y}$, $\vec{r}_t = x\hat{x} + y\hat{y}$, $\vec{r}_{t_o} = x_o\hat{x} + y_o\hat{y}$, $d\vec{k}_t = dk_x dk_y$, and $dv_o = dx_o dy_o dz_o$. We define the curly bracketed part of the kernel as $\tilde{\vec{A}}(\vec{k}_t)$.

Substituting $\vec{A}(\vec{r})$ in equation (A1) and interchanging the curl operators with the integral we obtain,

$$\vec{E}(\vec{r}) = \frac{-j\eta}{k_o(2\pi)^2} \int_{-\infty}^{\infty} \int_{-\infty}^{\infty} \nabla \times \left(\nabla \times \left[exp\left[-j\vec{k}_t \cdot \vec{r}_t - jKz\right] \tilde{\vec{A}}(\vec{k}_t) \right] \right) \, dk_x dk_y.$$

Using the vector identity $\nabla \times (\alpha \vec{V}) = \alpha(\nabla \times \vec{V}) - \vec{V} \times \nabla\alpha$, and noting that $\tilde{\vec{A}}(\vec{k}_t)$ is not a function of $\vec{r}$, we see the first term of our identity is zero, giving;

$$\vec{E}(\vec{r}) = \frac{-j\eta}{k_o(2\pi)^2} \int_{-\infty}^{\infty} \int_{-\infty}^{\infty} \nabla \times \left[\, \tilde{\vec{A}}(\vec{k}_t) \times (jk_x\hat{x} + jk_y\hat{y} + jK\hat{z}) \; exp\left[-j\vec{k}_t \cdot \vec{r}_t - jKz\right] \, \right] \, dk_x dk_y.$$

The above mentioned vector identity can be used again along with $(\vec{L}\times\vec{M})\times\vec{N} = (\vec{N}\cdot\vec{L})\vec{M} - (\vec{N}\cdot\vec{M})\vec{L}$ to reduce the integral further to,

$$\vec{E}(\vec{r}) = \frac{-j\eta k_o}{(2\pi)^2}\int_{-\infty}^{\infty}\int_{-\infty}^{\infty}\left[\tilde{\vec{A}}(\vec{k}_t) - (\hat{k}\cdot\tilde{\vec{A}}(\vec{k}_t))\hat{k}\right] exp\left[-j\vec{k}_t\cdot\vec{r}_t - jKz\right] dk_x dk_y,$$

with $\hat{k} = \dfrac{(jk_x\hat{x} + jk_y\hat{y} + jK\hat{z})}{k_o}$. This integral can be written in the form

$$\vec{E}(\vec{r}) = \frac{1}{(2\pi)^2}\int_{-\infty}^{\infty}\int_{-\infty}^{\infty}\vec{f}(k_x,k_y)\, exp\left[-j\vec{k}_t\cdot\vec{r}_t - jKz\right] dk_x dk_y, \qquad \text{(A3)}$$

where $\vec{f}(k_x,k_y) = -j\eta k_o\left[\tilde{\vec{A}}(\vec{k}_t) - (\hat{k}\cdot\tilde{\vec{A}}(\vec{k}_t))\hat{k}\right]$.

Setting $z = 0$ in equation (A3) we see that $\vec{E}(\vec{r})\,|_{\vec{r}=\vec{r}_t}$ is just the inverse Fourier transform of $\vec{f}_t$. Therefore, to find $\vec{f}_t$ we simply take the Fourier transform of the tangential field of the source at z = 0, see Figure A1. The surface is assumed to close at $r = \infty$ in the -z half space and obey a radiation condition. The resulting integral is

$$\vec{f}_t(k_x,k_y) = \int_{-\infty}^{\infty}\int_{-\infty}^{\infty}\vec{E}_t(\vec{r}_t,0)\, exp\left[jk_x x + jk_y y\right] dxdy \;=\; \mathfrak{F}\left\{\vec{E}_t(\vec{r}_t,0)\right\}.$$

To find f_z we use Gauss's equation for a charge free, homogeneous medium, namely $\nabla\cdot\vec{E} = 0$. The f_z component can be shown to be:

$$f_z = \frac{(-k_x f_x - k_y f_y)}{K}.$$

Finally, the radiated field off the source aperture in the region $z>0$ can be written as;

$$\vec{E}(\vec{r}) = \frac{1}{(2\pi)^2}\int_{-\infty}^{\infty}\int_{-\infty}^{\infty}\{\, f_x\hat{x} + f_y\hat{y} + f_z\hat{z}\,\}\, exp\left[-jk_x x - jk_y y - jKz\right] dk_x dk_y,$$

where $f_x = \mathfrak{F}\{E_x(\vec{r}_t,0)\}$, $f_y = \mathfrak{F}\{E_y(\vec{r}_t,0)\}$, and $f_z = \dfrac{(-k_x f_x - k_y f_y)}{K}$.

For the work in this thesis we need to know the incident magnetic field on a rough surface. To find the magnetic field off the source we use Faraday's law, given as $-j\omega\mu\vec{H} = \nabla \times \vec{E}$. Formally interchanging the curl and the integral, we see that the the curl operator acts on the exponential part of the integrand. The resulting equation for $\vec{H}$ is

$$\vec{H}(\vec{r}) = \frac{-1}{k_o \eta (2\pi)^2} \int_{-\infty}^{\infty}\int_{-\infty}^{\infty} \Big\{ \Big(\frac{k_y(k_x f_x + k_y f_y)}{K} + K f_y \Big)\, \hat{x} - \Big(K f_x + \frac{k_x(k_x f_x + k_y f_y)}{K} \Big)\, \hat{y} + \Big(-k_x f_y + k_y f_x \Big)\, \hat{z} \Big\}\, exp\big[-jk_x x - jk_y y - jKz\big]\, dk_x dk_y \qquad \text{(A4)}$$

for $z>0$. This equation will be used in subsequent appendices for calculation of the radiation pattern off a source having a Gaussian taper.

APPENDIX B: FRESNEL SOLUTION TO RADIATION

The following is a derivation of the radiated field given the source distribution $\vec{E}(\vec{r}_t) = exp\left[-\frac{x^2+y^2}{W^2}\right]\{A\hat{x}+B\hat{y}\}$ in the $z=0$ plane. The scattered field from a flat PEC will also be calculated assuming this radiated field is incident upon the surface and $k_o z_d \gg 1$, where z_d is the distance from the source plane to the PEC (see Figure B1). We start with the plane wave spectral representation of $\vec{H}$ given $\vec{E}_t$ in the $z=0$ plane. From Appendix A, equation (A4),

$$\vec{H}(\vec{r}) = \frac{-1}{k_o\eta(2\pi)^2}\int_{-\infty}^{\infty}\int_{-\infty}^{\infty}\left\{\left(\frac{k_y(k_x f_x + k_y f_y)}{K} + K f_y\right)\hat{x}\right.$$

$$- \left(K f_x + \frac{k_x(k_x f_x + k_y f_y)}{K}\right)\hat{y}$$

$$\left. + \left(-k_x f_y + k_y f_x\right)\hat{z}\right\} \exp\{-jk_x x - jk_y y - jKz\}\, dk_x dk_y, \quad \text{(B1)}$$

where $K = \sqrt{k_o^2 - (k_x^2 + k_y^2)}$, $f_x = \mathfrak{F}\{E_x(\vec{r}_t,0)\}$, and $f_y = \mathfrak{F}\{E_y(\vec{r}_t,0)\}$.

With $k_o z_d \gg 1$, we perform a binomial approximation on K, where K can be written $k_o\sqrt{1 - \frac{(k_x^2+k_y^2)}{k_o^2}}$. The physical implications of this approximation are that the spectrum is highly concentrated in the z direction. The approximation results in the following:

$$K \approx k_o - \frac{1}{2k_o}(k_x^2 + k_y^2)$$

and

$$K^{-1} \approx \frac{1}{k_o}\left(1 + \frac{1}{2k_o^2}(k_x^2 + k_y^2)\right).$$

By substituting the approximation of K and K^{-1} into equation (B1) we obtain,

$$\vec{H}(\vec{r}) = \frac{-1}{k_o \eta (2\pi)^2} \int_{-\infty}^{\infty} \int_{-\infty}^{\infty} \Big\{ \Big(k_y (k_x f_x + k_y f_y)(\frac{1}{k_o} + \frac{1}{2k_o{}^3}(k_x{}^2 + k_y{}^2)) + (k_o - \frac{1}{2k_o}(k_x{}^2 + k_y{}^2))\, f_y \Big)\, \hat{x}$$

$$- \Big((k_o - \frac{1}{2k_o}(k_x{}^2 + k_y{}^2))\, f_x + k_x (k_x f_x + k_y f_y)(\frac{1}{k_o} + \frac{1}{2k_o{}^3}(k_x{}^2 + k_y{}^2)) \Big)\, \hat{y}$$

$$+ \Big(-k_x f_y + k_y f_x \Big)\, \hat{z} \Big\} \exp\{-jk_x x - jk_y y - j(k_o - \frac{1}{2k_o}(k_x{}^2 + k_y{}^2))z\}\, dk_x dk_y.$$

This integral can be integrated exactly by making the following change of variables to simplify the expression. Let $u = \frac{k_x}{k_o}$ and $v = \frac{k_y}{k_o}$. This results in

$$\vec{H}(\vec{r}) = \frac{-k_o{}^2}{\eta (2\pi)^2} \int_{-\infty}^{\infty} \int_{-\infty}^{\infty} \Big\{ \Big(v\,(u\, f_x + v\, f_y)\,(1 + \frac{(u^2+v^2)}{2}) + (1 - \frac{(u^2+v^2)}{2})\, f_y \Big)\, \hat{x}$$

$$- \Big((1 - \frac{(u^2+v^2)}{2})\, f_x + u(u\, f_x + v\, f_y)(1 + \frac{(u^2+v^2)}{2}) \Big)\, \hat{y}$$

$$+ \Big(-u\, f_y + v\, f_x \Big)\, \hat{z} \Big\} \; exp\{j \frac{k_o z}{2} (u^2 + v^2)\}$$

$$exp\{-juk_o x - jvk_o y - jk_o z\}\, du dv, \qquad \text{(B2)}$$

where f_x and f_y are now functions of u and v.

Expanding out the terms in the integrand results in the following form for $\vec{H}$:

$$\vec{H}(\vec{r}) = \frac{-k_o{}^2}{\eta (2\pi)^2} \int_{-\infty}^{\infty} \int_{-\infty}^{\infty} \Big\{ \Big(f_x (\frac{u^3 v}{2} + \frac{v^3 u}{2} + uv) + f_y (\frac{v^4}{2} + \frac{u^2 v^2}{2} + \frac{v^2}{2} - \frac{u^2}{2} + 1) \Big)\, \hat{x}$$

$$- \Big(f_x (\frac{u^4}{2} + \frac{u^2 v^2}{2} + \frac{u^2}{2} - \frac{v^2}{2} + 1) + f_y (\frac{u^3 v}{2} + \frac{v^3 u}{2} + uv) \Big)\, \hat{y}$$

$$+ \Big(-u\, f_y + v\, f_x \Big)\, \hat{z} \Big\} \; exp\{j \frac{k_o z}{2} (u^2 + v^2)\}$$

$$exp\{-juk_o x - jvk_o y - jk_o z\}\, du dv.$$

Each power of u and v can be generated by taking derivatives of the second exponential with respect to x or y. Therefore, we will only have to integrate f_x

and f_y multiplied by the exponential terms.

$$\vec{H}(\vec{r}) = \frac{-k_o{}^2 exp\{-jk_o z\}}{\eta(2\pi)^2}\Bigg[\Big\{\Big(\tfrac{1}{2}\frac{1}{(-jk_o)^4}\Big(\frac{\partial^4}{\partial x^3\partial y}+\frac{\partial^4}{\partial x\partial y^3}\Big) + \frac{1}{(-jk_o)^2}\frac{\partial^2}{\partial x\partial y}\Big)\,\hat{x}$$

$$-\Big(\tfrac{1}{2}\frac{1}{(-jk_o)^4}\Big(\frac{\partial^4}{\partial x^4}+\frac{\partial^4}{\partial x^2\partial y^2}\Big)+\tfrac{1}{2}\frac{1}{(-jk_o)^2}\Big(\frac{\partial^2}{\partial x^2}-\frac{\partial^2}{\partial y^2}\Big)+1\Big)\,\hat{y}$$

$$+\Big(\frac{1}{(-jk_o)}\frac{\partial}{\partial y}\Big)\,\hat{z}\Big\}$$

$$\int_{-\infty}^{\infty}\int_{-\infty}^{\infty} f_x\, exp\{j\,\tfrac{k_o z}{2}\,(u^2+v^2)\}exp\{-juk_o x - jvk_o y\}\,dudv$$

$$+\ \Big\{\Big(\tfrac{1}{2}\frac{1}{(-jk_o)^4}\Big(\frac{\partial^4}{\partial y^4}+\frac{\partial^4}{\partial x^2\partial y^2}\Big) + \tfrac{1}{2}\frac{1}{(-jk_o)^2}\Big(\frac{\partial^2}{\partial y^2}-\frac{\partial^2}{\partial x^2}\Big)+1\Big)\,\hat{x}$$

$$+\Big(\tfrac{1}{2}\frac{1}{(-jk_o)^4}\Big(\frac{\partial^4}{\partial x^3\partial y}+\frac{\partial^4}{\partial x\partial y^3}\Big)+\frac{1}{(-jk_o)^2}\frac{\partial^2}{\partial x\partial y}\Big)\,\hat{y}$$

$$+\Big(\frac{-1}{(-jk_o)}\frac{\partial}{\partial x}\Big)\,\hat{z}\Big\}$$

$$\int_{-\infty}^{\infty}\int_{-\infty}^{\infty} f_y\, exp\{j\,\tfrac{k_o z}{2}\,(u^2+v^2)\}exp\{-juk_o x - jvk_o y\}\,dudv\Bigg], \qquad \text{(B3)}$$

with $f_x = \mathfrak{F}\{E_x(\vec{r}_t,0)\}$ and $f_y = \mathfrak{F}\{E_y(\vec{r}_t,0)\}$. Defining two operators L_1 and L_2 as

$$L_1 = \Big\{\Big(\tfrac{1}{2}\frac{1}{(-jk_o)^4}\Big(\frac{\partial^4}{\partial x^3\partial y}+\frac{\partial^4}{\partial x\partial y^3}\Big) + \frac{1}{(-jk_o)^2}\frac{\partial^2}{\partial x\partial y}\Big)\,\hat{x}$$

$$-\Big(\tfrac{1}{2}\frac{1}{(-jk_o)^4}\Big(\frac{\partial^4}{\partial x^4}+\frac{\partial^4}{\partial x^2\partial y^2}\Big)+\tfrac{1}{2}\frac{1}{(-jk_o)^2}\Big(\frac{\partial^2}{\partial x^2}-\frac{\partial^2}{\partial y^2}\Big)+1\Big)\,\hat{y}$$

$$+\Big(\frac{1}{(-jk_o)}\frac{\partial}{\partial y}\Big)\,\hat{z}\Big\}$$

and

$$L_2 = \left\{ \left(\frac{1}{2} \frac{1}{(-jk_o)^4} \left(\frac{\partial^4}{\partial y^4} + \frac{\partial^4}{\partial x^2 \partial y^2} \right) + \frac{1}{2} \frac{1}{(-jk_o)^2} \left(\frac{\partial^2}{\partial y^2} - \frac{\partial^2}{\partial x^2} \right) + 1 \right) \hat{x} \right.$$

$$+ \left(\frac{1}{2} \frac{1}{(-jk_o)^4} \left(\frac{\partial^4}{\partial x^3 \partial y} + \frac{\partial^4}{\partial x \partial y^3} \right) + \frac{1}{(-jk_o)^2} \frac{\partial^2}{\partial x \partial y} \right) \hat{y}$$

$$\left. + \left(\frac{-1}{(-jk_o)} \frac{\partial}{\partial x} \right) \hat{z} \right\},$$

respectively, we can write

$$\vec{H}(\vec{r}) = \frac{-k_o{}^2 exp\{-jk_o z\}}{\eta (2\pi)^2} \left\{ L_1 \int_{-\infty}^{\infty} \int_{-\infty}^{\infty} f_x \; exp\{ j \frac{k_o z}{2} (u^2 + v^2) \} exp\{-juk_o x - jvk_o y\} \; du dv \right.$$

$$\left. + L_2 \int_{-\infty}^{\infty} \int_{-\infty}^{\infty} f_y \; exp\{ j \frac{k_o z}{2} (u^2 + v^2) \} exp\{-juk_o x - jvk_o y\} \; du dv \right\}. \qquad \text{(B4)}$$

For our source, f_x and f_y are given as

$$f_x = A \; \pi \; W^2 \; exp\left[\left(-\frac{k_o{}^2 W^2}{4} \right) (u^2 + v^2) \right]$$

and

$$f_y = B \; \pi \; W^2 \; exp\left[\left(-\frac{k_o{}^2 W^2}{4} \right) (u^2 + v^2) \right],$$

respectively. The forms of f_x and f_y are easily combined with the quadratic phase terms in the integrand of (B4). The resulting integrals can be carried out analytically.

$$\vec{H}(\vec{r}) = \frac{-k_o{}^2 exp\{-jk_o z\}}{\eta (2\pi)^2} \{ AL_1 + BL_2 \} \left(\frac{\pi^2 W^2}{\alpha} exp\left[-\frac{k_o{}^2}{4\alpha} (x^2 + y^2) \right] \right), \qquad \text{(B5)}$$

where $\alpha = \left(\frac{k_o{}^2 W^2}{4} - \frac{jk_o z}{2} \right)$. Examining L_1 and L_2, we will keep only the constant term. The derivatives will bring down terms which are $O(\frac{1}{\alpha^2})$ and higher. These terms will be insignificant. With $z = z_d$, the field incident on the flat PEC can be written as (we have transformed form source to surface coordinates and $\theta_i = 0$)

$$\vec{H}_i(\vec{r}_{t_o}) = \frac{-k_o{}^2 W^2 \, exp\left[-jk_o z_d\right]}{\eta \, 4 \, \alpha} exp\left[-\frac{k_o{}^2}{4\,\alpha}(x_o{}^2 + y_o{}^2)\right]\left\{-A\,\hat{y}_o - B\,\hat{x}_o\right\}, \tag{B6}$$

where $\alpha = \left(\frac{k_o{}^2 W^2}{4} - \frac{jk_o z_d}{2}\right)$.

The current density induced on the surface is given exactly, for a flat PEC, by $\vec{J}_s(\vec{r}_o) = 2\ \hat{z}_o \times \vec{H}_i(\vec{r}_{t_o})$. Substituting this current into the integral for the scattered magnetic field and using an approximate form of the Green's function,

$$\vec{H}(\vec{r}) = \frac{k_o{}^2 W^2 \, exp\left[-jk_o z_d\right]}{\eta \, 2 \, \alpha} - jk_o \frac{exp\left[-jk_o r_r\right]}{4\pi r_r} \hat{k}_s \times (-A\,\hat{x}_o + B\,\hat{y}_o)$$

$$\int_{-\infty}^{\infty}\int_{-\infty}^{\infty} exp\left[-\frac{k_o{}^2}{4\,\alpha}(x_o{}^2 + y_o{}^2)\right] exp\left[jk_o \hat{k}_s \cdot \vec{r} - \frac{jk_o r_o^2}{2r_r}\right] dx_o dy_o$$

where r_r is distance to receiver and $\hat{k}_s$ is the direction of the observation point. In spherical coordinates $\hat{k}_s = \sin\theta\cos\phi\ \hat{x}_o + \sin\theta\sin\phi\ \hat{y}_o + \cos\theta\ \hat{z}_o$; therefore

$$\vec{H}(\vec{r}) = \frac{k_o{}^2 W^2 \, exp\left[-jk_o z_d\right]}{\eta \, 2 \, \alpha} - jk_o \frac{exp\left[-jk_o r_r\right]}{4\pi r_r} \hat{k}_s \times (-A\,\hat{x}_o + B\,\hat{y}_o)$$

$$\int_{-\infty}^{\infty}\int_{-\infty}^{\infty} exp\left[-\frac{k_o{}^2}{4\,\alpha}(x_o{}^2 + y_o{}^2)\right]$$

$$exp\left[jk_o(\sin\theta\cos\phi\ x_o + \sin\theta\sin\phi\ y_o - \frac{jk_o(x_o^2 + y_o^2)}{2r_r}\right] dx_o dy_o. \tag{B7}$$

Combining the quadratic phase terms, equation (B7) becomes:

$$\vec{H}(\vec{r}) = \frac{-jk_o{}^3 W^2 \, exp\left[-jk_o z_d - jk_o r_r\right]}{\eta \, 8\pi r_r \, \alpha} \hat{k}_s \times (-A\,\hat{x}_o + B\,\hat{y}_o)$$

$$\int_{-\infty}^{\infty}\int_{-\infty}^{\infty} exp\left[-\left(\frac{k_o{}^2}{4\,\alpha} + \frac{jk_o}{2r_r}\right)(x_o{}^2 + y_o{}^2)\right]$$

$$exp[jk_o(\sin\theta\cos\phi\ x_o + \sin\theta\sin\phi\ y_o)]\, dx_o dy_o$$

Carrying out this integration results in the following form for the $\vec{H}$ field off the

flat PEC.

$$\vec{H}(\vec{r}) = \frac{-jk_o{}^3W^2\ exp\left[-jk_oz_d - jk_or_r\right]}{\eta\ 8\pi r_r\alpha}\ \hat{k}_s \times (-A\ \hat{x}_o + B\ \hat{y}_o)$$

$$\frac{\pi}{\left(\frac{k_o{}^2}{4\ \alpha} + \frac{jk_o}{2r_r}\right)}\ exp\left[-\frac{\sin^2\theta}{4\left(\frac{k_o^2}{4\ \alpha} + \frac{jk_o}{2z_d}\right)}\right],$$

where $\alpha = \left(\frac{k_o{}^2W^2}{4} - \frac{jk_oz_d}{2}\right)$. To find the field back at the source, we note that $r_r = \sqrt{x^2+y^2+z_d^2}$. Since our initial incident field was found in a paraxial form we will simplify the above result as follows: $r_r \approx z_d$ in all terms except the linear phase term where $r_r = \sqrt{x^2+y^2+z_d^2} \approx z_d + \frac{x^2+y^2}{2z_d}$ and $\sin^2\theta \approx \frac{(x^2+y^2)}{z_d^2}$. As a consequence,

$$\vec{H}(\vec{r}) = \frac{jk_o{}^3W^2\ exp\left[-jk_o2z_d - jk_o\frac{x^2+y^2}{2z_d}\right]}{\eta\ 8\pi z_d\ \alpha}\ (A\ \hat{y}_o + B\ \hat{x}_o)$$

$$\times \frac{\pi}{\left(\frac{k_o{}^2}{4\ \alpha} + \frac{jk_o}{2z_d}\right)}\ exp\left[-\frac{(x^2+y^2)}{4z_d^2\left(\frac{k_o^2}{4\ \alpha} + \frac{jk_o}{2z_d}\right)}\right] \qquad \text{(B8)}$$

From image theory the field back up at the source aperture should be,

$$\vec{H}_i(\vec{r}_{t_o}) = \frac{k_o{}^2W^2\ exp\left[-jk_o2z_d\right]}{\eta\ 4\ \alpha}\ exp\left[-\frac{k_o{}^2}{4\ \alpha}(x^2+y^2)\right]\left\{A\ \hat{y}_o + B\ \hat{x}_o\right\},$$

where $\alpha = \left(\frac{k_o{}^2W^2}{4} - \frac{jk_o2z_d}{2}\right)$. If we factor the quadratic phase term into its real and imaginary parts, we obtain

$$\vec{H}_i(\vec{r}_{t_o}) = \frac{{k_o}^2 W^2 \, exp\left[-jk_o 2z_d\right]}{\eta \, 4 \, \alpha} exp\left[- \frac{\left({k_o}^2 W^2\right)}{\left({k_o}^2 W^4 + 16 z_d^2\right)} (x^2 + y^2) \right]$$

$$exp\left[\frac{jk_o z_d}{\left(\left(\frac{{k_o}^2 W^4}{4}\right) + 4z_d^2\right)} (x^2 + y^2) \right] \left\{ A \, \hat{y}_o + B \, \hat{x}_o \right\}.$$

The above result from image theory does agree with equation (B8). It is noteworthy to understand that if the quadratic phase term for the field off the surface had not been preserved, the result would not reduce to the same answer given by image theory. This is true no matter how far we move the source aperture away from the surface. Therefore we will attempt in this thesis to preserve the quadratic phase as much as can be possibly done.

APPENDIX C: FAR FIELD SOLUTION TO RADIATION

In this section we will derive the far field radiation pattern for a source field distribution of the form $\vec{E}_t = exp\left[-\frac{x^2+y^2}{W^2}\right]\{A\hat{x}+B\hat{y}\}$ in the $z=0$ plane. This analysis will be performed under the constraint that $k_o r \gg 1$, (whereas in Appendix B, we assumed $k_o z_d \gg 1$). To accomplish this, we will recall the exact result for calculating the $\vec{H}$ field given an aperture distribution using the plane wave spectrum approach:

$$\vec{H}(\vec{r}) = \frac{-1}{k_o \eta (2\pi)^2} \int_{-\infty}^{\infty}\int_{-\infty}^{\infty} \Big\{ \Big(\frac{k_y(k_x f_x + k_y f_y)}{K} + K f_y \Big)\hat{x} - \Big(K f_x + \frac{k_x(k_x f_x + k_y f_y)}{K} \Big)\hat{y} + \Big(-k_x f_y + k_y f_x \Big)\hat{z} \Big\} exp\big[-jk_x x - jk_y y - jKz\big]\, dk_x dk_y \tag{C1}$$

for $z>0$ and $K = \sqrt{k_o^2 - k_x^2 - k_y^2}$.

A general form for a multivariate integral, which is amenable to a stationary phase solution is of the form [22]

$$\hat{I}_n(\Omega) = \int_{-\infty}^{\infty} \cdots \int_{-\infty}^{\infty} f(\mathbf{x})\, exp[i\Omega q(\mathbf{x})]\, dx_1 \cdots dx_n, \qquad \text{where } \Omega > 0 \text{ and } \mathbf{x} = (x_1, \ldots, x_n).$$

For large Ω the asymptotic solution is given by [22]

$$\hat{I}_n(\Omega) \sim f(\mathbf{x}_S)\, exp[i\Omega q(\mathbf{x}_S)] \left(\frac{2\pi}{\Omega}\right)^{\frac{n}{2}} \frac{exp[i(\pi/4)\sigma]}{|\det(\partial^2 q/\partial x_{is}\partial x_{js})|^{\frac{1}{2}}}, \tag{C2}$$

where $\mathbf{x}_S = (x_{1s}, \ldots, x_{ns})$ are the simple zeros of $\frac{\partial q}{\partial x_i}$ with $i = 1,\ldots,n$ and $\sigma = \sum_{i=1}^{n} \text{sgn } d_i$, with d_i being the eigenvalues of the matrix with elements $\partial^2 q/\partial x_{is}\partial x_{js}$ for $i, j = 1, \ldots, n$.

Examining the argument of the exponential in equation (C1), and rewriting it in polar coordinates we have

$$k_x x + k_y y + Kz = rk_o\left(\frac{k_x}{k_o}\sin\theta\cos\phi + \frac{k_y}{k_o}\sin\theta\sin\phi + \sqrt{1-\left(\frac{k_x}{k_o}\right)^2-\left(\frac{k_y}{k_o}\right)^2}\cos\theta\right). \quad \text{(C3)}$$

Since we wish to investigate the situation in which $k_o r \gg 1$, we define $\Omega = k_o r$. The zeros of the derivative of (C3), the stationary phase points, are found to be (using Mathematica$_{©}$, [14,18]) $k_x = k_o\sin\theta\cos\phi$ and $k_y = k_o\sin\theta\sin\phi$. We also find $\mid \det(\partial^2 q/\partial x_{is}\partial x_{js}) \mid^{\frac{1}{2}} = \frac{1}{k_o\cos\theta}$ and $\sigma = -2$. The quantity $f(\mathbf{x}_s)$, is simply the multiplier of the exponential term of equation (C1) with k_x and k_y evaluated at the stationary phase points given above. For a more in depth discussion of asymptotic solutions, see [23].

For the source aperture with distribution $\vec{E}_t = exp\left[-\frac{x^2+y^2}{W^2}\right]\{A\hat{x}+B\hat{y}\}$ in the $z = 0$ plane, we find from Appendix B that

$$f_x = A\,\pi\,W^2\,exp\left[\left(-\frac{W^2}{4}\right)(k_x{}^2+k_y{}^2)\right] \text{ and } f_y = B\,\pi\,W^2\,exp\left[\left(-\frac{W^2}{4}\right)(k_x{}^2+k_y{}^2)\right].$$

Evaluating these expressions at the stationary phase points and making the appropriate substitutions into (C2) using (C1) results in

$$\vec{H} = \frac{-jW^2\,k_o}{\eta 2r}\,exp[-jk_o r]\,exp\left[-\frac{k_o{}^2W^2}{4}\sin^2\theta\right]\cos\theta$$
$$\Big\{(\tan\theta\sin\theta(\sin\phi\cos\phi\ A+\sin^2\phi\ B)+\cos\theta\ B)\ \hat{x}$$
$$-(\tan\theta\sin\theta(\cos^2\phi\ A+\sin\phi\cos\phi\ B)+\cos\theta\ A)\ \hat{y}$$
$$+(\sin\theta(-\cos\phi\ B\ +\sin\phi\ A))\ \hat{z}\Big\}.$$

Since $\frac{k_o{}^2W^2}{4} \gg 1$, we evaluate the amplitude terms at $\theta = 0$, and use the binomial approximations on the decay and phase terms. Setting $r = z$ in the

denominator, results in.

$$\vec{H} = \frac{-jW^2 k_o}{\eta 2z} exp\left[- jk_o z - jk_o \frac{(x^2+y^2)}{2z} \right] exp\left[- \frac{k_o{}^2 W^2}{4} \frac{(x^2+y^2)}{z^2} \right] \left\{ B\ \hat{x} - A\ \hat{y} \right\}. \qquad (C4)$$

The incident field on the PEC which is $z = z_d$ away from the source aperture, is, therefore,

$$\vec{H} = \frac{jW^2 k_o}{\eta 2 z_d} exp\left[-jk_o z_d - jk_o \frac{(x_o{}^2+y_o{}^2)}{2z_d} \right] exp\left[- \frac{k_o{}^2 W^2}{4} \frac{(x_o{}^2+y_o{}^2)}{z_d{}^2} \right] \left\{ B\ \hat{x}_o + A\ \hat{y}_o \right\}.$$

Using the above field as the incident field on a flat PEC, the scattered field can be found. The exact current density on the surface is given by $\vec{J}_s(\vec{r}_{t_o}) = 2\ \hat{z} \times \vec{H}_i$. Putting this into the integral for the magnetic vector potential, results in the following for $\vec{A}(\vec{r})$:

$$\vec{A}(\vec{r}) = \frac{jW^2 k_o\ exp\left[- jk_o z_d \right]}{\eta\ z_d} \left\{ - A\ \hat{x}_o + B\ \hat{y}_o \right\} \int_{-\infty}^{\infty} \int_{-\infty}^{\infty} exp\left[\left(- \frac{k_o{}^2 W^2}{4\ z_d{}^2} - \frac{jk_o}{2z_d} \right) (x_o{}^2 + y_o{}^2) \right]$$

$$\cdot G\ dx_o dy_o.$$

Here, $G = \dfrac{exp\left[- jk_o \sqrt{(x-x_o)^2 + (y-y_o)^2 + z^2} \right]}{4\pi \sqrt{(x-x_o)^2 + (y-y_o)^2 + z^2}}$.

Since the integrals in their present form are intractable, we use the $k_o z \gg 1$ assumption, and approximate the Green's function by

$$G = \frac{1}{4\pi z} exp\left[- jk_o z \left(1 + \frac{(x-x_o)^2 + (y-y_o)^2}{2z^2} \right) \right]$$

This results in

$$\vec{A}(\vec{r}) = \frac{jW^2 k_o \, exp\left[-jk_o(z_d+z)\right]}{\eta 4\pi \, z_d \, z} \hat{e} \, exp\left[-\frac{jk_o}{2z}(x^2+y^2)\right]$$

$$\int_{-\infty}^{\infty}\int_{-\infty}^{\infty} exp\left[-\left(x_o^2+y_o^2\right)\left(\frac{k_o^2 W^2}{4z_d^2}+\frac{jk_o}{2z}+\frac{jk_o}{2z_d}\right)\right]$$

$$\cdot exp\left[\frac{jk_o}{z}(xx_o+yy_o)\right] dx_o dy_o, \qquad \text{(C5)}$$

where $\hat{e} = \left\{-A\,\hat{x}_o + B\,\hat{y}_o\right\}$.

Using the integral identity [19] $\int_{-\infty}^{\infty} exp\left[-at^2+bt\right] dt = \left(\frac{\pi}{a}\right)^{\frac{1}{2}} exp\left[\frac{b^2}{4a}\right]$, for Re[$a$] >0, equation (C5) yields,

$$\vec{A}(\vec{r}) = \frac{jW^2 k_o \, exp\left[-jk_o(z_d+z)\right]}{\eta 4\pi \, z_d \, z} \hat{e} \, exp\left[-\frac{jk_o}{2z}(x^2+y^2)\right] \frac{\pi}{\gamma} \, exp\left[-\frac{k_o^2(x^2+y^2)}{z^2 \, 4\gamma}\right]$$

where $\gamma = \left(\frac{k_o^2 W^2}{4z_d^2}+\frac{jk_o}{2z}+\frac{jk_o}{2z_d}\right)$.

If we evaluate this at $z = z_d$, it does not exactly equal the source radiation equation (C4) simply evaluated at $z = 2z_d$. However, if we enforce some conditions we are able to recover the result produced by image theory. Rewriting γ such that $\gamma = \frac{jk_o}{z_d}\left(\frac{-jk_o W^2}{4z_d}+1\right)$ and using the assumption that $\frac{k_o W^2}{4} \ll z_d$ allows us to approximate γ by $\gamma \approx \frac{jk_o}{z_d}$ and $\gamma^{-1} \approx \frac{z_d}{jk_o}\left(1+\frac{jk_o W^2}{4z_d}\right)$. Substituting this for $\vec{A}(\vec{r})$, we obtain

$$\vec{A}(\vec{r}) = \frac{jW^2 k_o \, exp\left[-jk_o 2z_d\right]}{\eta 4 \, z_d^2 \, \frac{jk_o}{z_d}} \hat{e} \, exp\left[-\frac{jk_o}{2z_d}(x^2+y^2)\right]$$

$$\cdot exp\left[-\frac{k_o^2(x^2+y^2)}{z_d^2 \, 4} \, \frac{z_d}{jk_o}\left(1+\frac{jk_o W^2}{4z_d}\right)\right].$$

Simplifying this expression results in

$$\vec{A}(\vec{r}) = \frac{W^2\, exp\left[-jk_o 2z_d\right]}{\eta 4\, z_d}\, \hat{e}\, exp\left[-\frac{jk_o}{4z_d}(x^2+y^2)\right] exp\left[\frac{-k_o{}^2 W^2}{16\, z_d{}^2}(x^2+y^2)\right].$$

Taking the curl of $\vec{A}$ to get $\vec{H}$ results in,

$$\vec{H}(\vec{r}) = \frac{-jk_o W^2\, exp\left[-jk_o 2z_d\right]}{\eta 4\, z_d}\, \hat{p}\, exp\left[-\frac{jk_o}{4z_d}(x^2+y^2)\right] exp\left[\frac{-k_o{}^2 W^2}{16\, z_d{}^2}(x^2+y^2)\right],$$

where $\hat{p} = \left\{-B\, \hat{x}_o - A\, \hat{y}_o\right\}$.

Evaluating (C4) at $z = 2z_d$, matches the result above. The imposition of $\frac{k_o W^2}{4z_d} \ll 1$, along with $k_o r \gg 1$ and $k_o z \gg 1$ in the Green's Function brings the two forms into agreement. If we rewrite the assumption $\frac{k_o W^2}{4z_d} \ll 1$ in terms of the electromagnetic wavelength, we get $z_d \gg \frac{\pi W^2}{2\lambda}$, the very familiar constraint for the far field. Since we neglect all inverse powers of z^2 and higher in computing the radiated $\vec{H}$ field, it is consistent that the far field condition would bring these two solutions into agreement.

APPENDIX D: SURFACE STATISTICS

In the evaluation of fields scattered by random rough surfaces, a priori knowledge of the surface statistics must be available. There are many forms of single point probability density functions that might be used [3]. However, for probability density functions (pdf) of order three or higher, the multivariate Gaussian is used due to the fact that there are no other pdf's available. The general form of the Gaussian pdf is given as[24];

$$\text{pdf}(x_1,x_2,x_3,\ldots,x_n)= \frac{1}{|\,C\,|^{1/2}(2\pi)^{n/2}} exp\Big[-\tfrac{1}{2}\,U^T\,C^{-1}\,U\Big]$$

where U= column matrix of the variables $(x_1,x_2,x_3,\ldots,x_n)$

U^T= transpose of U

C= covariance matrix defined as $E[U\ U^T]$

n= number of random variables.

In this thesis we investigate a homogeneous, isotropic surface with a zero mean height. The correlation function for the heights is assumed to be Gaussian. We assume that the single point heights and slopes will be uncorrelated. For Gaussian statistics this implies that the height and slope are independent at a single point.

The correlation function for the random heights at two points for this thesis will be represented by the function R. As was mentioned earlier, this correlation function is assumed to be Gaussian. The specific form is given by,

$$R(\Delta x,\Delta y)=\langle\zeta_o^2\rangle\ exp\left[-\frac{(\Delta x^2+\Delta y^2)}{l^2}\right],$$

where l is the two point correlation length, and $\langle\zeta_o^2\rangle$ is the variance of the surface heights.

When we form the covariance matrix it will be necessary to differentiate R with respect to Δx and Δy. We will now define the following notation for these derivatives.

$$R_y = \frac{\partial}{\partial \Delta y} R = -\frac{2\langle \zeta_o^2 \rangle}{l^2} \Delta y \, exp\left[-\frac{(\Delta x^2 + \Delta y^2)}{l^2} \right]$$

$$R_{yy} = \frac{\partial^2}{\partial \Delta y^2} R = -\frac{2\langle \zeta_o^2 \rangle}{l^2} \left(1 - \frac{2\Delta y^2}{l^2} \right) exp\left[-\frac{(\Delta x^2 + \Delta y^2)}{l^2} \right].$$

We can form then, the covariance matrix which is required to complete the averaging of the field quantities. The implications of the isotropic nature of the surface, which are utilized in Appendix E, are that the correlation function is only a function of the distance between two surface points and not the direction. This will allow us to decrease the number of integrations for our plane wave illumination check case.

APPENDIX E: PLANE WAVE INCIDENT KIRCHHOFF NRCS

Using the Kirchhoff approximation, we will derive in this appendix the NRCS of a rough PEC when illuminated by an infinite plane wave. The incident electric field will be given by the following (in the surface coordinate system):

$$\vec{E}_i = \left\{ -A\ \hat{x}_o + B\ (C_\theta \hat{y}_o + S_\theta \hat{z}_o) \right\} exp\left[-jk_o(y_o S_\theta - \zeta_o C_\theta + z_d) \right]. \qquad (E1)$$

Finding the far field radiation from the surface when illuminated by this field, can be accomplished through,

$$\vec{E}_s = \frac{jk_o\eta}{2\pi r_r} exp[-jk_o r_r]\, \hat{k}_s \times \left(\hat{k}_s \times \int_{-\infty}^{\infty} \int_{-\infty}^{\infty} \left[-\hat{x}_o \left\{ \zeta_{y_o} A S_\theta + A C_\theta \right\} + \hat{y}_o \left\{ \zeta_{x_o} A S_\theta + B \right\} \right.\right.$$

$$\left.\left. + \hat{z}_o \left\{ -\zeta_{x_o} A C_\theta + \zeta_{y_o} B \right\} \right] K\ exp\left[jk_o \hat{k}_s \cdot \vec{r}_o \right] dx_o dy_o. \qquad (E2)$$

with $K = \frac{1}{\eta}\ exp\left[-jk_o(y_o S_\theta - \zeta_o C_\theta + z_d) \right]$ and $\hat{k}_s \cdot \vec{r}_o = x_o \sin\theta\cos\phi + y_o\ \sin\theta\sin\phi + \zeta_o \cos\theta$. As we will use this to compare with the results of the Gaussian beam illumination, we must find the scattered field in the backscatter direction, specifically $\hat{k}_s = -S_\theta \hat{y}_o + C_\theta \hat{z}_o$.

Using this specific scattering direction and performing the cross products and simplifying yields

$$\vec{E}_s = \frac{-jk_o}{2\pi r_r} exp[-jk_o r_r] \int_{-\infty}^{\infty} \int_{-\infty}^{\infty} \left[-\hat{x}_o \left\{ \zeta_{y_o} A S_\theta + A C_\theta \right\} + \hat{y}_o \left\{ C_\theta S_\theta \zeta_{y_o} B + B\ C_\theta^2 \right\} \right.$$

$$\left. + \hat{z}_o \left\{ B S_\theta^2 \zeta_{y_o} + B S_\theta C_\theta \right\} \right] exp\left[-jk_o(2y_o S_\theta - 2\zeta_o C_\theta + z_d) \right] dx_o dy_o. \qquad (E3)$$

To find the NRCS, we use the following expression,

$$\sigma_i^o = \frac{4\pi r_r^2 \left(\langle \vec{E}_s \cdot \vec{E}_s^* \rangle - \langle \vec{E}_s \rangle \cdot \langle \vec{E}_s^* \rangle \right)}{\int_{-\infty}^{\infty} \int_{-\infty}^{\infty} |E_i|^2 ds_o}. \tag{E4}$$

Using the method described in [3],[6] and [13], we will determine the slope term averages by using differentiation of the phase term. This results in several "edge effect terms" in the integrand, which are assumed to cancel and yield no contribution. This is true when the surface is illuminated out to many correlation lengths, and in the case of infinite plane wave illumination this is obviously the case. The details of the differentiation will not be shown. The resulting expression for the normalized radar cross section of a random rough PEC under the Kirchhoff approximation is given as

$$\sigma_i^o = \frac{k_o^2}{\pi} F \int_0^{2\pi} \int_0^{\infty} \left\{ exp\left[-k_o^2 4 C_\theta^2 (\langle \zeta_o^2 \rangle - R) \right] - exp\left[-k_o^2 4 C_\theta \langle \zeta_o^2 \rangle \right] \right\} * exp\left[-j 2 k_o S_\theta \Delta r \, sin\psi \right] \Delta r d \Delta r d\psi. \tag{E5}$$

where $F = \sec^2 \theta_i$.

We can further simplify this expression by normalizing to a wavelength and integrating over ψ. The following expression results in

$$\sigma_i^o = 8\pi^2 \int_0^{\infty} F \left\{ exp\left[-k_o^2 4 C_\theta^2 (\langle \zeta_o^2 \rangle - R) \right] - exp\left[-k_o^2 4 C_\theta \langle \zeta_o^2 \rangle \right] \right\} J_o(4\pi S_\theta p) p dp. \tag{E6}$$

Equation (E6) was derived as a check for the Gaussian beam illumination case. As the beam illumination becomes larger and larger the NRCS should match that given in equation (E6), which is the result for a plane wave illumination. The graphs in the results and conclusions section all have this check case plotted.

APPENDIX F: NRCS DISCUSSION

Classically, the definition for the finite target radar cross section is given by,

$$\sigma = \lim_{r_r \to \infty} \frac{4\pi {r_r}^2 \, S_{scat}}{S_{inc}},$$

where S_{inc} is the power density incident on the target and S_{scat} is the power density arriving at the receiver. Due to the infinite surfaces being considered in random rough surface scattering the convention is to define a scattering cross section per unit area, given by

$$\sigma^o = \lim_{r_r \to \infty} \frac{4\pi {r_r}^2 \left(\langle \vec{E}_s \cdot \vec{E}^*{}_s \rangle - \langle \vec{E}_s \rangle \cdot \langle \vec{E}^*_s \rangle \right)}{A_{ill} E_o^2}.$$

This expression assumes that a plane wave illumination was used as the illuminating source for the rough surface scattering. When beam illumination is used as the illuminating field, a more general form for the normalized radar cross section (NRCS), must be used. The denominator now contains the integration over the entire mean surface to account for the total incident power. The NRCS is thus given by

$$\sigma^o = \lim_{r_r \to \infty} \frac{4\pi {r_r}^2 \left(\langle \vec{E}_s \cdot \vec{E}^*{}_s \rangle - \langle \vec{E}_s \rangle \cdot \langle \vec{E}^*_s \rangle \right)}{\int_{-\infty}^{\infty} \int_{-\infty}^{\infty} |E_i|^2 ds_o}.$$

It can easily be seen that for a plane wave illumination, $\vec{E}_i = \vec{E}_o exp[-jk_o z]$, the denominator becomes,

$$\int_{-\infty}^{\infty} \int_{-\infty}^{\infty} |E_i|^2 ds_o = \lim_{A_{ill} \to \infty} (A_{ill} |\vec{E}_o|^2).$$

Once again the distinction must be made, that we are illuminating infinite surfaces and therefore deal with a scattering cross section per unit area. For the Gaussian beam case we are defining this above as the NRCS. Multiplying the NRCS by the effective area will give the rcs as is the case for the plane wave illumination.

APPENDIX G: GAUSSIAN BEAM MULTIVALUED TAPER CONSIDERATIONS

As was mentioned in the Results and Conclusions section the Gaussian beam field incident on the random PEC has the same beam taper for two values of the source field radius W. The result we use for the incident field is closely linked to the solutions of the paraxial wave equation. Many authors have studied the solutions to the paraxial wave equation with the fundamental solution being the Gaussian beam[25]. Looking at the expressions derived by Haus[25], we see that the solutions for the Gaussian beam will in fact give the same value of beam radius at a constant distance, z, for two distinct source beam radii, W. This is shown for our incident field in figure 7.0; for normal incidence, with $z_d = 1000\lambda$ and the two values of W being 10λ and 31.85λ. The tapers being the same does not imply that the fields on the surface are the same. The phases associated with each of the two values of W are drastically different, as also shown in figure 7.0. The smaller value of the source field radius for figure 7.0, $W = 10\lambda$, has a much sharper increase in phase as a function of the surface radius, than the larger source field generates. The interpretation being that the larger source diffracts slower, due to its spectrum, and the phase will stay more planar. A smaller source looks more like a point source and has a more curved phase front.

Further investigation into this phenomenon may prove to gain insight into the region of validity of the solutions to the paraxial wave equation. The radiated fields do not satisfy zero divergence except close to the z-axis. This is another point of interest to investigate for paraxial wave solutions.

Vita

Keith Allen Tyeryar was born in Newport News, Virginia on August 28, 1967. He graduated from Tabb High School in 1985. He worked as a summer student at the Continuous Electron Beam Accelerator Facility (CEBAF), Newport News, Virginia, during the summers of 1986 and 1987. He completed his B.S. degree in Electrical Engineering from Virginia Polytechnic Institute and State University in 1989. He worked as a NASA Langley Research Summer Scholar during the summers of 1989 and 1990. His interest lie in random surface scattering, radio wave propagation, and antenna theory. He is also an amateur radio operator, call sign KD4LQQ.